MARSOL

Demonstrating Managed Aquifer Recharge as a Solution to Water Scarcity and Drought

Physical (Sandbox) Modelling of Melides Demo Site

Deliverable No.	D12.5
Version	1.0
Version Date	11.10.2016
Author(s)	Teresa E. Leitão, Tiago Martins, Maria José Henriques, J.P. Lobo Ferreira and João Rogeiro (all LNEC, besides the cooperation of Ana Maria Carmen from University of Ferrara) (LNEC)
Dissemination Level	PU
Status	Final

Contents

Figures

Tables

1. INTRODUCTION

Workpackage 12 deals with modelling MAR solution's implementation. To study the effectiveness of these solutions, Task 12.5 was conceived and developed using physical models - which represent the real case study sites in a small and controlled scale - to demonstrate the effectiveness of MAR, namely clogging issues and physic-chemical treatment of recharging water.

Besides the physico-chemical treatment, the experiments were also numerically modelled with the same tools used to model the real cases, and in cooperation with Workpackage 14.

To develop Task 12.5, a new physical sandbox model was built in LNEC's modelling facilities (cf. http://www.lnec.pt/en/research/research-infrastructures/fluvial-hydraulics-experimental-facility/) under MARSOL project. The artificial aquifer facility (or physical sandbox model) can be used to conduct laboratory large scale infiltration and tracer tests, aiming to determine the soil infiltration rate and also the contaminants retention and/or degradation capacity, namely to simulate Soil-Aquifer Treatment (SAT) in a Managed Aquifer Recharge (MAR) basin.

The DEMO site PT3 – Melides aquifer, river and lagoon (Alentejo) was selected to model and demonstrate soil-aquifer-treatment (SAT-MAR) to remove rice paddy field pollutants prior to their discharge into Melides lagoon. The results obtained in these tests gave the necessary knowledge to build, in the future, an *in situ* SAT-MAR facility.

2. DEMO SITE PT3 – MELIDES CHARACTERISATION

2.1 MOTIVATION FOR THE SITE SELECTION

Melides lagoon MARSOL case-study area was selected based on the following background considerations and advantages:

1. This is an area where relevant environmental quality problems (agriculture contamination) arise during the summer period, due to the rejection of nitrates and pesticides in Melides coastal lagoon from rice paddy fields (Leitão *et al.*, 2012 and Lobo Ferreira *et al.*, 2013).
2. A relevant amount of surface and groundwater data, including climate change water budget and groundwater recharge estimations is available, having been gathered during the Portuguese FCT sponsored PROWATERMAN project http://www.lnec.pt/hidraulica-ambiente/pt/projectos/detalhe/prowaterman-agua-ecossistemas-aquaticos-e-atividade-humana-uma-abordagem-integrada-e-participativa-na-definicao-de-estrategias-inovadoras-e-prospetivas-de-gestao-integrada-de-recursos-hidricos-no-s/).
3. A regional groundwater flow model has been developed by LNEC during PROWATERMAN project, allowing simulating real time aquifer responses, by MARSOL partner LNEC for the Melides aquifer.
4. Following the PROWATERMAN Final Workshop, organized by LNEC both in Alentejo, at the University of Évora and in Grândola Municipality, MARSOL project actor APA Ambiente is supporting Melides MARSOL research and case-study objectives.

Aiming to contribute to solve the water quality problems due to the agriculture activities, the use of soil aquifer treatment (SAT) basins was envisaged. By infiltrating some of the rejections from the paddy fields wastewater in basins with appropriate MAR INNO-DEMO solutions, an improvement of the water quality can be expected.

For this purpose, the Melides soils were studied, first in soil-column experiments (Section 3.4) and then using a physical sand box model (Sections 4 and 5).

2.2 MELIDES BRIEF CHARACTERIZATION

2.2.1 Location

Melides lagoon is the terminal part of the watershed area of Melides river, located in the Alentejo coast, and overlying Sines aquifer system (Figure 1). This coastal lagoon rarely opens to the ocean, usually through infrequent episodes of short duration, being dependent on the ocean agitation, tides, storms and rainfall. However, the lagoon is artificially opened by APA Ambiente, usually once a year.
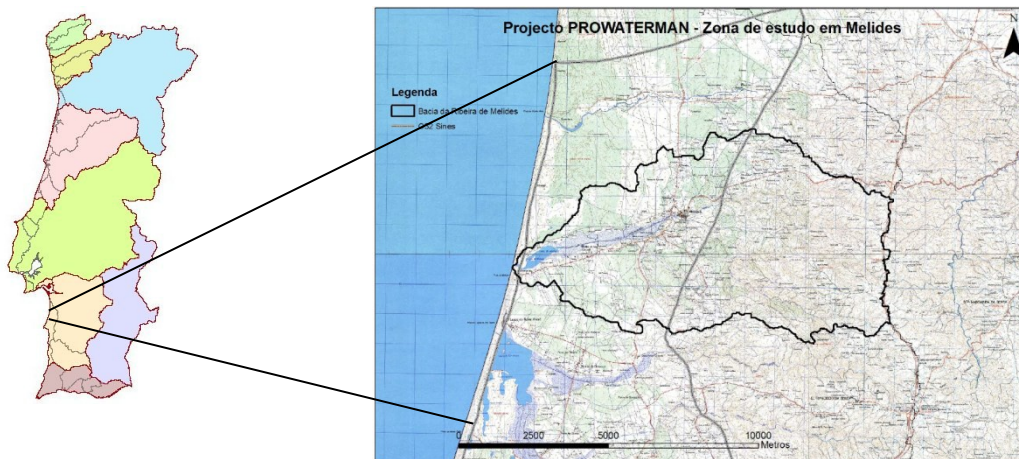
Figure 1 – PT3 Melides DEMO site (Oliveira *et al*., 2012)

2.2.2 Hydrography and hydrogeology

The 60.84 km^2 Melides hydrographic basin may be divided in two different sectors (Monteiro *et al*., 2008; Novo and Oliveira, 2014): the upstream sector, with greater relief, developed on low permeability formations of Palaeozoic schists and greywackes; and the downstream sector, of plain relief inducing low to moderate drainage density, which is developed in Cenozoic sandy formations that overlay Jurassic carbonate units, belonging to the Sines aquifer system. The two sectors are separated by Santo André's fault.

Surface flow dominates in the upstream sector, being reduced in the downstream sector to only a few streams that mainly transport surface flow generated in the upstream sector. Groundwater recharge predominates in the downstream sector. In the downstream sector the connection between the drainage network and the deep carbonate aquifer is made solely by the *Fonte dos Olhos* spring; in the rest of the sector only the upper aquifer is in direct connection with the drainage network that receives the discharge water of the aquifer.

Melides lagoon is located downstream in the hydrographic basin and constitutes a coastal ecosystem partially dependent on groundwater (Lobo Ferreira *et al.*, 2013). It is a receptor of the total amount of pollutant load of surface origin collected by the drainage network of the Melides stream and also of the pollutant load of groundwater flow that discharges to the surface water network or directly to the lagoon.

2.2.3   Water budget balance

The Melides lagoon has an annual average volume of water of 1.6 hm^3, receiving a volume of about 20 hm^3, of which 14 hm^3/year come from runoff (11.2 hm^3/year coming from upstream in the river basin sector and 2.8 hm^3/year downstream sector) and above 5 hm^3 from the upper aquifer from the downstream zone of the basin (Oliveira *et al.* 2012). Thus, the volume that the lagoon receives annually is about 12.5 times its average value and should be a significant renewal of lagoon water (Novo *et al.*, 2013).

The average recharge in the basin is about 119 mm/year (Figure 2) and the direct runoff is 199 mm/year (Oliveira and Oliveira, 2012). In the downstream area of the basin (area dominated by Tertiary deposits) direct the flow is 100 mm/year, in the rice paddy fields area 150 mm/year to 200 mm/year. In terms of water contributing to the lagoon, 56 to 60% comes from the runoff of the upstream basin, 27% comes from the discharge of the aquifer in the downstream zone of the basin (which corresponds to about 95% of the clearance of this area) and 13.5% from the runoff originated in the same downstream zone (Oliveira *et al.*, 2012).
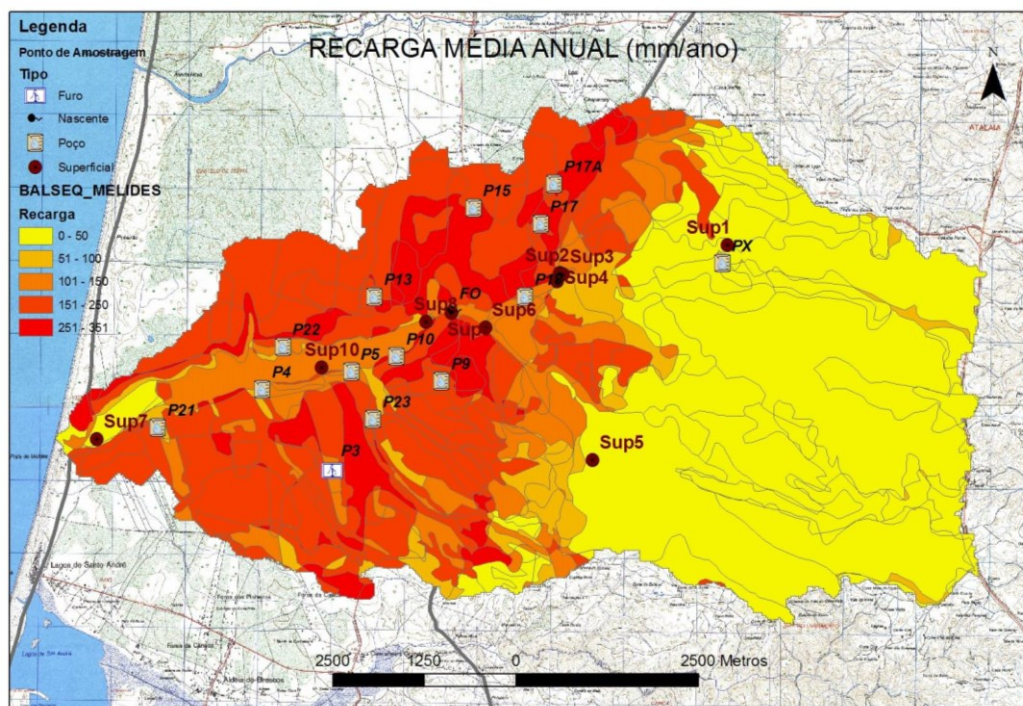
Source: Oliveira *et al.* (2012)

Figure 2 – Average annual recharge at Melides

Thus, given the importance of groundwater proportion that reaches the pond, it was established as a partially dependent on groundwater ecosystem. The groundwater quality has a major importance in the ecosystem good functioning.

3. SOIL CHARACTERISATION

3.1 SOIL COMPOSITION

The composition of Melides soil was analysed in LNEC U3M laboratory using X-Ray (Figure 3). It aimed to see its natural characteristics and ability for existing pollutants retention or degradation.
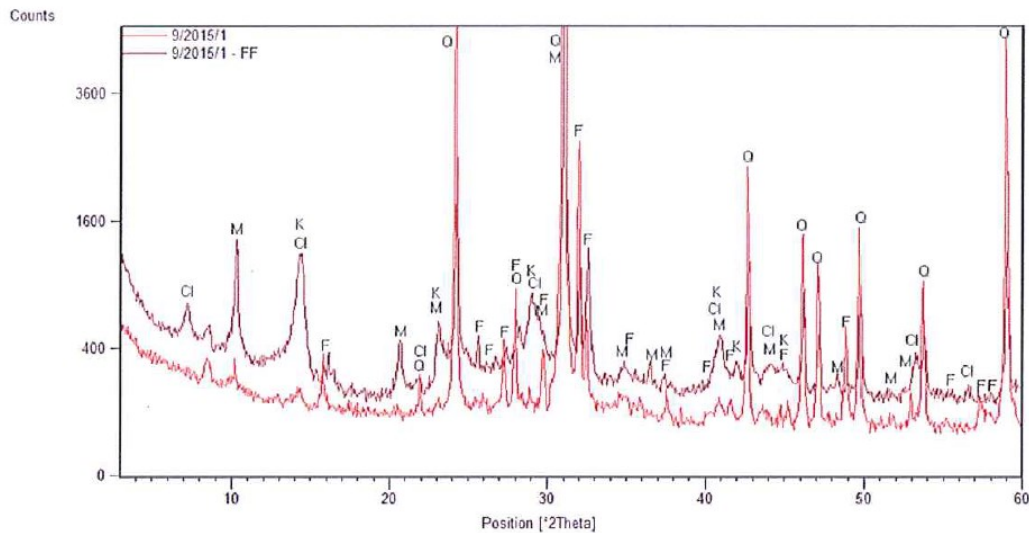
Figura 1 – Registos difratométricos da amostra 9/2015/1 (tal qual e < 63 µm). Notação utilizada: Cl – clorite; M – mica; K – caulinite; F – feldspatos; Q – quartzo.

Figure 3 – Results from X-Ray diffractometry for Melides soil (9/2015/1) and the fine fraction of Melides soil (9/2015/1) - FF

The results show that the minerals in:

- higher proportion are: quartz (SiO_2) and alkaline feldspars [microcline - (K, Na)$AlSi_3O_8$ and albite - $NaAlSi_3O_8$];

- lower proportion are: mica (illite – $KAl_2Si_3AlO_{10}.OH_2$), chlorite ($(Mg,Fe)_6(Si,Al)_4O_{10}(OH)_8$) and kaolinite ($Al_2Si_2O_5(OH)_4$).

3.2 SOIL BULK DENSITY

Melides soil bulk density is 1.59 g/cm^3. It has been determined by dividing the weight of a dry soil sample (after 72 hours of drying in an oven at temperature 50°C) (934 g) by the volume the soil occupied in a cylindrical sampler (588.75 cm^3):

$$\rho_b = W_{dry} / V_{cup}$$ **Equation 1**

where:

ρ_b – soil dry bulk density (g/cm^3)
W_{dry} – weight of dry soil sample (g)
V_{cup} – volume occupied by sample (cm^3)

3.3 POROSITY

For porosity determination, soil samples have been dried in an oven at 50°C for 72 hours. Then water has been added and samples have been left for complete saturation for 72 hours. Porosity of studied soils has been calculated by dividing the volume of water in a saturated soil sample by the volume of the soil-column:

$$n = V_w / V_{tot}$$ **Equation 2**

where:

n – porosity;
V_w – volume of water in soil sample (cm^3) $\equiv W_{sat}$ - W_{dry};
W_{sat} – weight of saturated soil sample (g);
W_{dry} – weight of dry soil sample (g);
V_{tot} – volume occupied by sample (cm^3).

The calculated porosity value is 0.38 (0.38 = 222.04 cm^3 / 588.75 cm^3).

3.4 PERMEABILITY

A set of soil-column experiments were conducted in May and June 2014 to determine the hydraulic conductivity of Melides soils.

The laboratory setup consists of a PEAD column with 30 cm height and 5 cm diameter with a weight support attached for soil compaction. The column was filled with the soil, which was previously dried at 40°C and the visible organic matter removed (roots, leaves, etc.), following the CEN/Technical Specification 14405 (2004) instructions. The column was completely saturated from the bottom and the experiment started with continuous flow from the top using an automatic peristaltic pump.
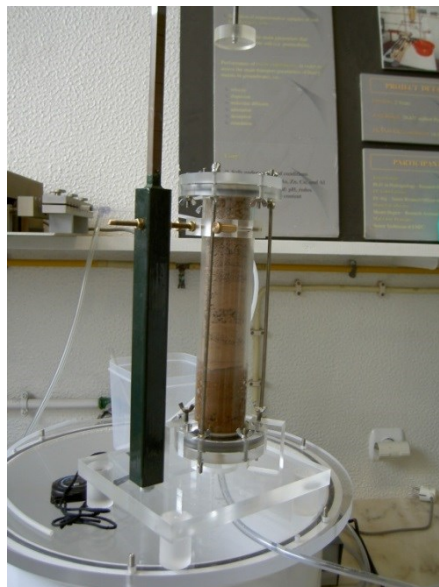
Figure 4 – Column experiment with saturation from the bottom

Results obtained allowed concluding that the soil has permeability values adequate for SAT, with an average Darcy permeability ranging from 0.9 to 4.8 m/d at Melides, the latter for a 20-30 cm layer where permeability increase significantly.

4. PHYSICAL (SANDBOX) MODEL

4.1 POTENTIALITIES AND AIM

The artificial aquifer facility (or physical sandbox model) was built under MARSOL project and used to conduct laboratory large scale infiltration and tracer tests, both for saturated and non-saturated conditions. They allow determining the soil:

- infiltration rate, in full saturation conditions;

- contaminants retention and/or degradation capacity.

For MARSOL experiments, this facility was used to study Soil-Aquifer Treatment (SAT) simulating a Managed Aquifer Recharge (MAR) infiltration basin.

Additionally, this same facility can be used to simulate other situations such as:

- risk of contaminants leaching from a spill;

- reactive barriers for groundwater rehabilitation;

- contaminants release from a contaminated porous material.

4.2 SANDBOX CONSTRUCTION AND DESCRIPTION

The physical sandbox model was built during 2015/16 in LNEC hydraulics pavilion area (http://www.lnec.pt/en/research/research-infrastructures/fluvial-hydraulics-experimental-facility/). This facility is approx. 3.5 m long, 1 m wide and 2 m high (Figure 5) and can be filled with the porous medium (soil) to be studied, in this case the Melides sand.

Figure 5 – LNEC physical (sandbox) model construction

The area can be divided in up to three different compartments to perform simultaneous experiments (Figure 6). The facility was equipped with three piezometers, Teflon cups to sample the vadose zone and monitoring devices such as multiparametric probes (water pressure, pH, temperature, electrical conductivity and redox) to monitor flow and transport, both in the saturated and vadose zones.

Figure 6 – LNEC physical (sandbox) model sections, A, B and C

4.3 EXPERIMENTAL SETUP

4.3.1   Sandbox set-up

Aiming to model and demonstrate the use of soil-aquifer-treatment (SAT) basins as a tool to remove rice paddy fields pollutants, prior to their discharge in Melides lagoon, the sandbox model was used to perform three simultaneous experiments with Melides soil.

The sandbox model was divided into three sections (Figure 7) to test the adsorption and degradation capacity of the following different soil mixtures:

- **Section A** – Melides soil in all the vertical profile;

- **Section B** – 30 cm top layer of a mixture of Melides soil (60%) and vegetal compost (40% with 65% organic matter, i.e. the mixture has 26% of OM), followed by Melides soil in the remaining depth; and

- **Section C** – two layers of the same vegetal compost about 3 cm separated by 17 cm of Melides soil, followed by Melides soil in the remaining depth.

Figure 8 presents a schematic diagram of the sandbox model dimensions and the soil profiles referred to above.

Figure 7 – Detail of three soil layers being tested simultaneously (left) and the external piezometer (right)

Section	Description
A	Natural soil only
B	Mixed soil (40% organic, 60% nat) 30 cm layer
C	Two organic layers of 3 cm separated by 17 cm of natural soil

Section	Area (m²)	Volume (m³)
A	1.0925	2.245088
B	1.0925	2.2287
C	0.96425	1.957428
Total	3.14925	6.431215
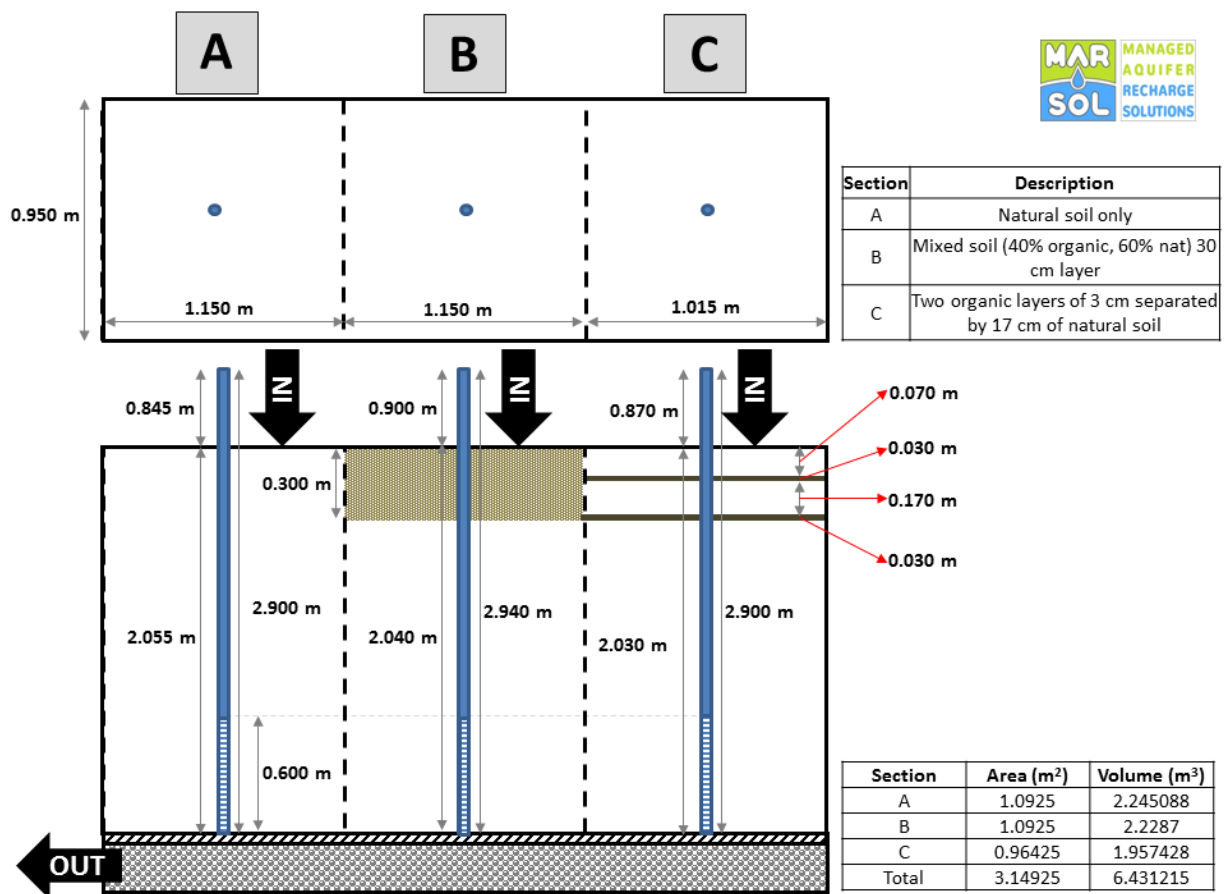
Figure 8 – Schematic diagram of the physical (sandbox) model dimensions and soil mixtures used in MARSOL SAT experiments

4.3.2   Materials

To analyse the behaviour of the tracers along their infiltration path in the soil profile, and to assess the different behaviour of the three soil mixtures, the following monitoring devices were installed in each section: A, B and C (Figure 10):

- Two Prenart capsules (Figure 9) in the vadose zone, at two depths, 30 cm and 60 cm.
- One piezometer with continuous *in situ* reading of T, EC, water level (and discrete analysis of pH and redox).
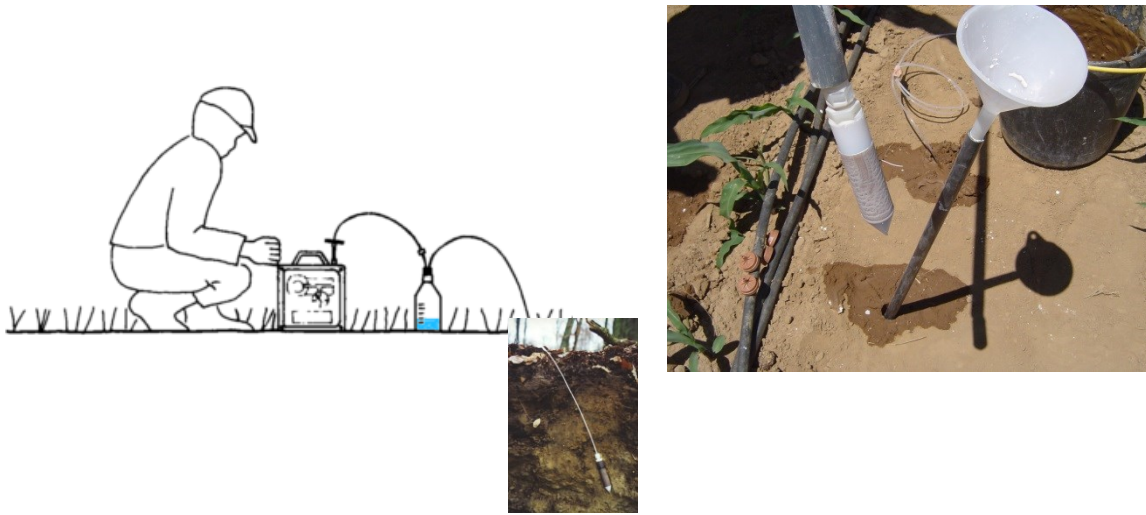
Figure 9 – Vadose zone monitoring devices used in the physical (sandbox) model

To sample the vadose zone water, the air inside the bottle (Figure 9) needed to be sucked with a peristaltic pump. This process allows sampling at the desired depth.

Figure 10 – *In situ* monitoring devices, both for the saturated and vadose zones

4.3.3   Methodology

Tracer selection

In each section (A, B and C), two tracer experiments (Experiment 1 and 2), with spiked fertilizer and hydrocarbons, were performed in May/June 2016 to analyse the adsorption and degradation capacity of the three different soil mixtures. Experiment 1 was a pulse injection and Experiment 2 was a continuous injection (with the tracer deposited on the top of the soil). The fertilizer selected corresponds to a common chemical fertilizer. The more important concentrations for the plant growth (not including all elements, so the sum is not 100%) are referred by the producer as: N (12%), P_2O_5 (12%), K_2O (17%), Cl (0.9%), MgO (2%), as well as very small percentages of sulphur, boron and zinc.

Furthermore, a NaCl conservative tracer was added to help identifying the increase in electrical conductivity (EC) and, with that, the more adequate sampling periods.

Experiment 1

Experiment 1 was performed from May 31st to June 1st 2016.

Experiment 1 was performed by flooding the soil surface with 0.5 m^3 of water. The <u>tracer volume</u> was determined in order to correspond to approximately 20% of the soil basin total pore volume (2.45 m^3), considering the three section's volumes (Table 1) and the calculated soil average porosity (section 3.3). The 500 L were spread using 20 plastic bottles with 25 L capacity (cf. Figure 11).

Figure 11 – Bottles used to store the tracer for the physical (sandbox) model Experiment 1

Table 1 – Physical sandbox compartment's dimensions

Section	Length (m)	Width (m)	Height (m)	Area (m^2)	Volume (m^3)	Pore volume (m^3), considering 38% porosity
A	1.15	0.95	2.06	1.09	2.25	0.85
B	1.15	0.95	2.04	1.09	2.23	0.85
C	1.02	0.95	2.03	0.96	1.96	0.74
Total	3.32	2.85	6.13	3.15	6.43	2.45

The average flowrate (Q) measured in the outflow before the experiment was 0.063 L/s, i.e. 5.44 m^3/d, corresponding to a velocity V (Q/Area) of 1.73 m/d and a pore velocity (V/n) of 4.55 m/d. Although this value was not obtained for full saturation conditions, it is equivalent to the values measured in laboratory for saturated conditions (see Section 3.4). Considering the 2.45 m^3 sandbox pore volume, it takes about 10.8 hours for a complete PV to flow throughout the sandbox (or each 24 hours about 2.22 PV is percolated in the sandbox).

The <u>tracer concentration</u> in the spiked tracer water was calculated in order to correspond to 2 times the typical dose advised for most horticultural species, i.e. 2 x 500 kg/ha. The overall tracer concentration and weight were calculated for the 500 L, divided by the three sections (Table 2).

Table 2 – Fertilizer tracer concentration calculation for Experiment 1

Section	Tracer volume m^3 (20% PV)	Number of 25 L bottles	Tracer concentration (1000 kg/ha)	Tracer concentration (mg/L)	Tracer (g)	N (mg/L) N, 12%	P_2O_5 (mg/L) P_2O_5, 12%	K (mg/L) K_2O, 17%	Cl (mg/L) Cl, 0.9%	Mg (mg/L) MgO, 2%
A	0.17	7	0.092	53.62	9.153	6.43	6.43	3.78	4.83	0.65
B	0.17	7	0.092	54.01	9.153	6.48	6.48	3.81	4.86	0.65
C	0.15	6	0.104	69.67	10.371	8.36	8.36	4.92	6.27	0.84
Total	0.49	20	0.032	6.49	28.677	0.78	0.78	0.46	0.58	0.08

For the hydrocarbons, the tracer (diesel) concentration was defined to be a value 15 times higher than the 0.5 mg/L detection limit used for the chemical analysis, i.e. 7 mg/L. NaCl concentration was chosen in order to make to a clear increase in the water electrical conductivity. This corresponds to 500 mg/L. Table 3 presents the calculations for the tracer's weight.

Table 3 – Total Hydrocarbon (HC) and NaCl tracer concentration calculation for Experiment 1

Section	Tracer volume (m^3) (20% PV)	Number of 25 L bottles	HC Tracer concentration (mg/L)	HC Tracer (g)	NaCl Tracer concentration (mg/L)	NaCl Tracer (g)
A	0.17	7	7	1.195	500	85.361
B	0.17	7	7	1.186	500	84.738
C	0.15	6	7	1.042	500	74.424
Total	0.49	20	21	3.423	1500	244.524

Experiment 2

Experiment 2 was performed after finishing Experiment 1, from June 1st to June 3rd 2016.

For the Experiment 2, the same amount of tracer was used, but the tracer was applied in powder on the top of the soil (Figure 12). In this way the tracer release was much slower. No hydrocarbons were used.

Figure 12 – Tracer grains on the top of the soil from the physical (sandbox) model, Experiment 2

4.4 MONITORING

To analyse the behaviour of the different soil mixtures simulating SAT treatment, the following sampling protocol was defined for both experiments (cf. Table 4 and Table 5):

- vadose zone: six devices (two depths and three compartments) for water sampling;

- piezometers: three devices (one well and three compartments) for water quality sampling and continuous monitoring of *in situ* T, EC, pH, redox;

- soil: six areas (two depths, 30 cm and 60 cm, and three compartments), for Experiment 1.

Table 4 – Sampling protocol for the Experiment 1

MAR SOL	Sampling protocol for the physical (sandbox) model															
Sample #1 2016/05/30	**# Sampling devices**	**Water**								**Soil**					
		NO_3^-	NO_2^-	NH_4^+	Ca, Na, Mg, K	SO_4^{2-}	Cl	HCO3	HC	NO_3^-	NO_2^-	NH_4^+	PO_4^{3+}	SO_4^{2-}	HC
Vadose - basin															
Wells	3	x	x	x		x	x	x	x						
Infiltration water	1	x	x	x	x	x	x	x	x						
Soil															
Sample #2 to sample #7	**# Sampling devices**	**Water**								**Soil**					
		NO_3^-	NO_2^-	NH_4^+	Ca, Na, Mg, K	SO_4^{2-}	Cl	HCO3	HC	NO_3^-	NO_2^-	NH_4^+	PO_4^{3+}	SO_4^{2-}	HC
Vadose - basin															
Wells	3	x	x	x		x	x	x	x						
Infiltration water															
Soil															
Sample #8	**# Sampling devices**	**Water**								**Soil**					
		NO_3^-	NO_2^-	NH_4^+	Ca, Na, Mg, K	SO_4^{2-}	Cl	HCO3	HC	NO_3^-	NO_2^-	NH_4^+	PO_4^{3+}	SO_4^{2-}	HC
Vadose - basin	6	x	x	x		x	x	x	x						
Wells	3	x	x	x		x	x	x	x						
Infiltration water															
Soil															
Sample #9 to 17	**# Sampling devices**	**Water**								**Soil**					
		NO_3^-	NO_2^-	NH_4^+	Ca, Na, Mg, K	SO_4^{2-}	Cl	HCO3	HC	NO_3^-	NO_2^-	NH_4^+	PO_4^{3+}	SO_4^{2-}	HC
Vadose - basin															
Wells	3	x	x	x		x	x	x	x						
Infiltration water															
Soil															
Sample #18	**# Sampling devices**	**Water**								**Soil**					
		NO_3^-	NO_2^-	NH_4^+	Ca, Na, Mg, K	SO_4^{2-}	Cl	HCO3	HC	NO_3^-	NO_2^-	NH_4^+	PO_4^{3+}	SO_4^{2-}	HC
Vadose - basin	6	x	x	x	x	x	x	x	x						
Wells	3	x	x	x	x	x	x	x	x						
Infiltration water															
Soil	6									o	o	o	o	o	x
Legend:	x - samples to IST														
	o - samples to AmbiPar Control														

Table 5 – Sampling protocol for the Experiment 2

MAR SOL	Sampling protocol for the physical (sandbox) model								
Sample #19 to 20 2016/06/02 and 03	**# Sampling devices**	**Water**							
		NO_3^-	NO_2^-	NH_4^+	Ca, Na, Mg, K	SO_4^{2-}	Cl	HCO3	HC
Vadose - basin	6	x	x	x		x	x	x	x
Wells	3	x	x	x		x	x	x	x
Infiltration water									
Soil									
Legend:	x - samples to IST								

Furthermore, the spiked infiltration water was analysed at the beginning of the first experiment.

5. RESULTS AND CONCLUSIONS

5.1 EXPERIMENT 1

Experiment 1 was carried out during 24 hours, between 11 AM of May 31st to 11 AM of June 1st. Table 6 presents the main characteristics of Experiment 1 regarding the inflow, piezometric level and experiment timings.

The difference of water volume on the flowmeter between 17:57 (31-05-2016) and 8:20 (01-06-2016) is equivalent to an inflow value of 0.107 L/s (5.5 m^3 in 14h20 or 51600 sec) or 9.25 m^3/d. Considering the calculated pore volume (2.45 m^3, see Section 4.3.3), this means that water percolated during the whole experiment corresponds to approximately 3.8 times the pore volume of the physical sandbox model.

Table 6 – Main characteristics of Experiment 1

Date/time	Inflow (L/s)	Volume reading at counter (m^3)	Depth to the water table (m)	Notes
30-05-2016 11:50	0.096	10078.6	0	Inflow started to achieve steady state
30-05-2016 12:24	0.098	-	0	-
30-05-2016 16:38	0.092	-	0	-
30-05-2016 17:50	-	-	0.56	-
31-05-2016 11:00	-	-	-	Experiment 1 starts / tracer injection
31-05-2016 11:30	-	-	-	Tracer injection stops
31-05-2016 17:57	0.11	10089	0.87	-
01-06-2016 08:20	0.11	10094.5	0.8	-
01-06-2016 09:24	0.076	-	0.74	-
01-06-2016 11:00	-	-	-	Experiment 1 finishes / injection stops

Figure 13 presents the results obtained from the CTD diver concerning the depth to the water table and the electrical conductivity (EC). The figure shows a fast increase of the water table (decrease in the depth to the water table) after the tracer injection started which was extended for 1 hour after the tracer injection stopped. The water inflow during the remaining period of the experiment was tried to be kept constant, but some small oscillations in the water pressure have occurred. Nevertheless, the main reason for the water table decrease was due to the release of water in the outflow tap, done in order to balance the inflow with the outflow, while stabilizing the water table.

Concerning the electrical conductivity, Figure 13 shows the three peak (breakthrough curve maximum value) arrivals. It is possible to observe that the tracer arrived first to PzA and with higher EC values when compared to the tracer arrival in Section B and C, as a result of the higher retention capacity of Melides soil mixed with vegetal compost.
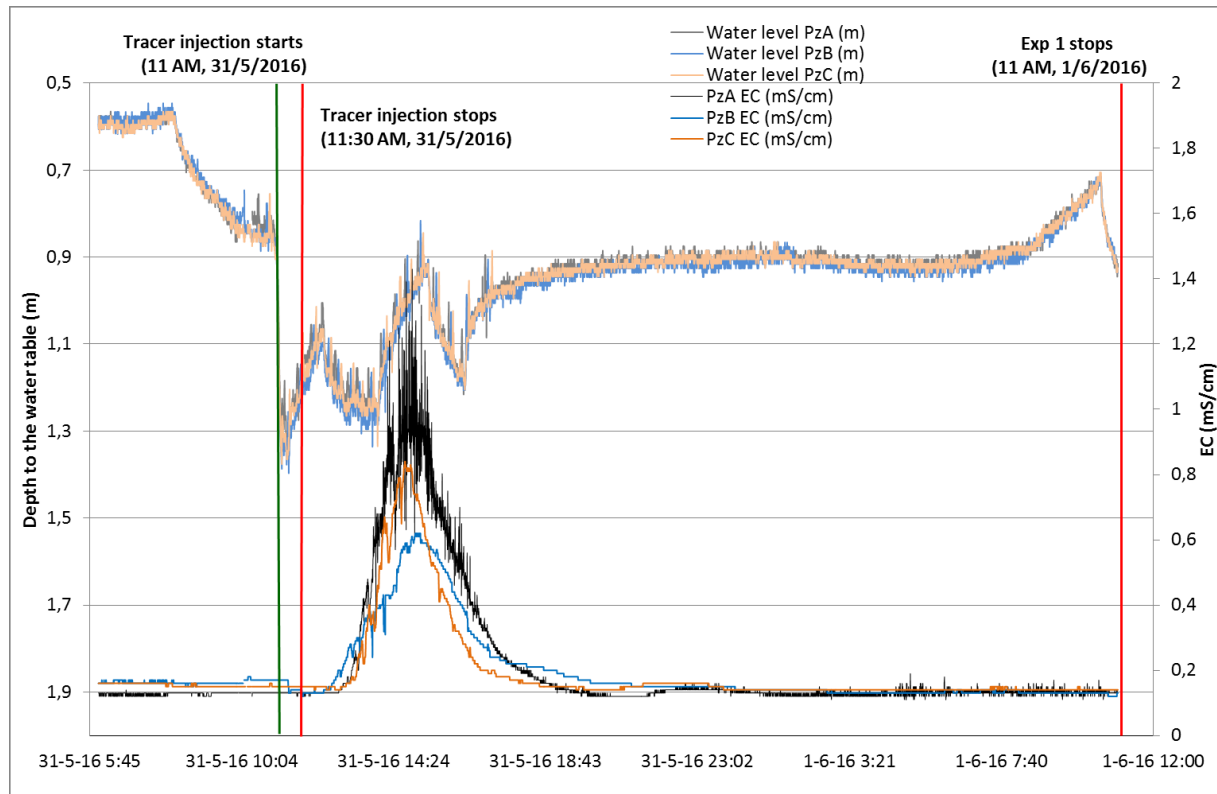
Figure 13 – Piezometric water level and electrical conductivity values in the three piezometers, Experiment 1

In addition to the continuous measurement with the CTD diver, several discrete samples were retrieved from the six vadose zone cups and the three piezometers during the whole experiment period. Table 7 presents the water quality concentrations results. In the first column, under "designation", the first letter represents the Section of the experiment (A, B or C), the subsequent number is the soil depth (30 or 60 cm) or GW if collected in the piezometers, and the last number is the sampling number.

Table 7 – Results from the chemical analysis of water samples collected during Experiment 1

Designation	Day Hour	NO_3^-	NO_2^-	NH_4^+	Ca^{2+}	Mg^{2+}	Na^+	K^+	SO_4^{2-}	Cl^-	HCO_3^-	HC
Units					mg/L							µg/L
Tracer 1	31-05 11:05	5.9	<0.01	3.7	18	3.1	180	6.9	27	275	53.8	78
Vadose cups												
A-30-1	31-05 13:26	4	<0.01	-	-	-	-	-	20	139	47.9	-
A-30-2	01-06 11:05	2.2	<0.01	0.9	-	-	-	-	13	31	52.2	-
A-60-1	31-05 13:30	3.2	<0.01	-	-	-	-	-	17	80	-	-
A-60-2	01-06 11:07	1.9	<0.01	0.46	-	-	-	-	11	10	52.3	160
Piezometers												
A-GW-1	31-05 10:57	2	<0.1	<0.05	18	4.3	9.3	3.2	11	9.4	54.1	<10
A-GW-2	31-05 11:20	1.9	<0.1	<0.05	-	-	-	-	11	9.3	48.1	11
A-GW-3	31-05 11:40	1.8	<0.1	<0.05	19	5.8	9.3	3.6	11	9.2	52.8	<10
A-GW-4	31-05 11:59	1.8	<0.1	<0.05	-	-	-	-	13	9.2	55.2	<10
A-GW-5	31-05 12:21	2.1	<0.1	<0.05	-	-	-	-	11	10	55.9	35
A-GW-6	31-05 12:43	2	<0.1	<0.05	-	-	-	-	10	18	53.5	<10

Designation	Day Hour	NO_3^-	NO_2^-	NH_4^+	Ca^{2+}	Mg^{2+}	Na^+	K^+	SO_4^{2-}	Cl^-	HCO_3^-	HC
A-GW-7	31-05 13:00	2.5	<0.01	<0.05	27	7.9	12	4.7	9.9	45	47.9	<10
A-GW-8	31-05 13:20	2.6	<0.01	<0.05	-	-	-	-	10	54	47.8	23
A-GW-9	31-05 13:40	3.5	<0.1	<0.05	-	-	-	-	11	93	44	20
A-GW-10	31-05 14:00	3.9	<0.01	<0.05	-	-	-	-	13	139	42.3	35
A-GW-11	31-05 14:21	4.9	<0.01	<0.05	-	-	-	-	19	210	45.8	56
A-GW-12	31-05 14:41	5.5	<0.01	<0.05	-	-	-	-	22	235	44.5	110
A-GW-13	31-05 15:02	5.8	<0.01	<0.05	-	-	-	-	27	248	35.9	130
A-GW-14	31-05 15:30	5	<0.01	<0.05	-	-	-	-	29	202	72.2	98
A-GW-15	31-05 15:55	4.2	<0.01	<0.05	-	-	-	-	28	145	84.9	110
A-GW-16	31-05 16:30	3.6	<0.1	<0.05	-	-	-	-	27	107	122	<10
A-GW-17	31-05 17:00	2.5	<0.1	<0.05	-	-	-	-	22	44	94.9	27
A-GW-18	01-06 11:00	1.8	<0.1	0.4	16	3.7	9.6	3.4	11	9.5	50.6	<10
Vadose cups												
B-30-1	31-05 13:31	3.6	<0.01	-	-	-	-	-	12	33	-	-
B-30-2	01-06 11:08	4.5	<0.01	<0.05	-	-	-	-	12	25	110	-
B-60-1	31-05 13:35	3.8	0.04	-	-	-	-	-	16	76	80.2	-
B-60-2	01-06 11:09	2.9	0.04	0.29	-	-	-	-	11	9.9	53.4	-
Piezometers												
B-GW-1	31-05 10:57	2.3	<0.1	<0.05	15	5.5	9.3	32	11	9.4	75.3	47
B-GW-2	31-05 11:25	2.4	<0.1	<0.05	-	-	-	-	11	9.3	78.5	37
B-GW-3	31-05 11:45	2.4	<0.1	<0.05	16	7.4	9.8	40	11	9.3	78.4	<10
B-GW-4	31-05 12:04	2.3	<0.1	<0.05	-	-	-	-	11	9.4	84.4	<10
B-GW-5	31-05 12:25	2.8	<0.1	<0.05	-	-	-	-	11	18	74.6	<10
B-GW-6	31-05 12:47	2.7	<0.1	<0.05	-	-	-	-	11	33	71.8	21
B-GW-7	31-05 13:05	3	<0.1	<0.05	28	7.9	15	36	12	53	70.3	<10
B-GW-8	31-05 13:24	3.6	<0.1	<0.05	-	-	-	-	13	86	64.7	20
B-GW-9	31-05 13:43	4	0.03	<0.05	-	-	-	-	15	108	62.3	29
B-GW-10	31-05 14:04	4.4	0.03	<0.05	-	-	-	-	17	140	37.9	<10
B-GW-11	31-05 14:23	5.2	0.05	<0.05	-	-	-	-	20	192	55.9	57
B-GW-12	31-05 14:44	5.7	0.04	<0.05	-	-	-	-	22	220	55.6	39
B-GW-13	31-05 15:05	6.4	0.07	<0.05	-	-	-	-	26	232	58.9	43
B-GW-14	31-05 15:32	6.7	0.04	<0.05	-	-	-	-	28	207	69.5	22
B-GW-15	31-05 15:58	6.1	0.24	<0.05	-	-	-	-	28	146	89	36
B-GW-16	31-05 16:33	5.1	<0.1	<0.05	-	-	-	-	23	79	111	22
B-GW-17	31-05 17:04	4.5	<0.1	<0.05	-	-	-	-	17	39	117	13
B-GW-18	01-06 11:08	2.8	<0.1	0.12	20	3.9	9.8	8.9	11	9.6	72.4	<10
Vadose cups												
C-30-1	31-05 13:35	4.3	0.03	-	-	-	-	-	19	127	63.1	-
C-30-2	01-06 11:13	2.4	0.04	0.65	-	-	-	-	11	13	39	63
C-60-1	31-05 13:39	-	-	-	-	-	-	-	-	-	-	-
C-60-2	01-06 11:15	4.8	0.08	-	-	-	-	-	-	48	-	-
Piezometers												
C-GW-1	31-05 10:57	2.1	<0.1	<0.05	18	4.2	8.6	14	11	9.3	66.7	<10
C-GW-2	31-05 11:30	2.1	<0.1	<0.05	-	-	-	-	11	9.2	63.2	<10
C-GW-3	31-05 11:50	2.1	<0.1	<0.05	20	6.5	9.3	12	11	9.3	67.8	<10
C-GW-4	31-05 12:10	2	<0.1	<0.05	-	-	-	-	11	9.4	66.9	<10
C-GW-5	31-05 12:35	2	<0.1	<0.05	-	-	-	-	11	9.4	66.4	<10

Designation	Day Hour	NO$_3^-$	NO$_2^-$	NH$_4^+$	Ca^{2+}	Mg^{2+}	Na$^+$	K$^+$	SO$_4^{2-}$	Cl$^-$	HCO$_3^-$	HC
C-GW-6	31-05 12:51	2.1	<0.1	<0.05	-	-	-	-	10	13	64	<10
C-GW-7	31-05 13:10	2.5	<0.1	<0.05	21	5.1	9.3	13	10	37	57.5	<10
C-GW-8	31-05 13:30	2.8	<0.1	<0.05	-	-	-	-	10	54	54.7	<10
C-GW-9	31-05 13:46	3.4	<0.01	<0.05	-	-	-	-	11	84	51.6	15
C-GW-10	31-05 14:07	4.6	<0.01	<0.05	-	-	-	-	18	163	49.1	18
C-GW-11	31-05 14:26	5.5	0.03	<0.05	-	-	-	-	23	210	50.9	12
C-GW-12	31-05 14:47	5.8	0.05	<0.05	-	-	-	-	26	211	57.7	19
C-GW-13	31-05 15:08	5.1	0.09	<0.05	-	-	-	-	26	145	75	12
C-GW-14	31-05 15:34	4.3	<0.1	<0.05	-	-	-	-	22	80	88.1	11
C-GW-15	31-05 16:05	4	<0.1	<0.05	-	-	-	-	20	62	91.1	16
C-GW-16	31-05 16:36	3.6	<0.1	<0.05	-	-	-	-	16	33	90.4	<10
C-GW-17	31-05 17:06	3.4	<0.1	<0.05	-	-	-	-	12	15	88.1	<10
C-GW-18	01-06 11:12	2.3	<0.1	0.14	20	3.5	9.7	5.2	11	9.5	63.3	<10

Figure 14 presents the breakthrough curves obtained in the saturated water from the piezometer installed in Section A.
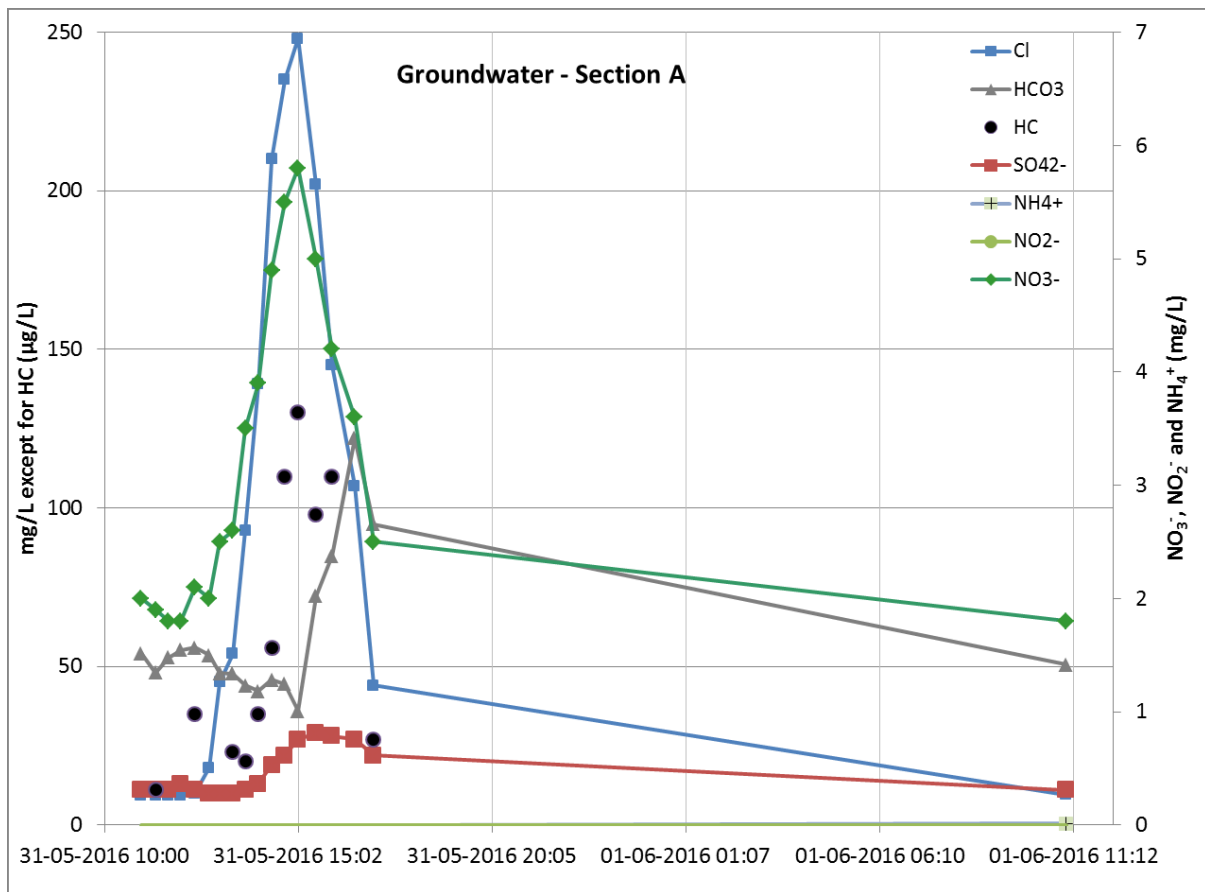
Figure 14 – Breakthrough curves obtained for the water samples from the Section A piezometer

The sharp and symmetrical curves obtained both for chloride (Cl$^-$) and nitrate (NO$_3^-$), together with the simultaneous peak arrival of both ions - in concentrations similar to the initial concentration of the tracer - confirms the inert character of Melides sand. Neither nitrite (NO$_2^-$) nor ammonia (NH$_4^+$)

was found in the piezometer water samples during the experiment. Possibly the NH_4^+ existing in the tracer (3.7 mg/L) was nitrified with the presence of oxygen:

$$2\ NH_4^+ + 3O_2 \rightarrow 2NO_2^- + 2H_2O + 4H^+ \qquad \text{Equation 3}$$

$$2NO_2^- + O_2 \rightarrow 2NO_3^- \qquad \text{Equation 4}$$

In fact, the samples collected in the vadose zone (Figure 15) show the presence of NH_4^+ in the water from 30 to 60 cm in the second day (the first day there was not enough water for analysis), in minor conditions when compared to the input of 3.7 mg/L, also with very little concentration arriving to the saturated zone. In the soil samples collected at two depths after the experiment, only nitrite and HC were found (Table 8).
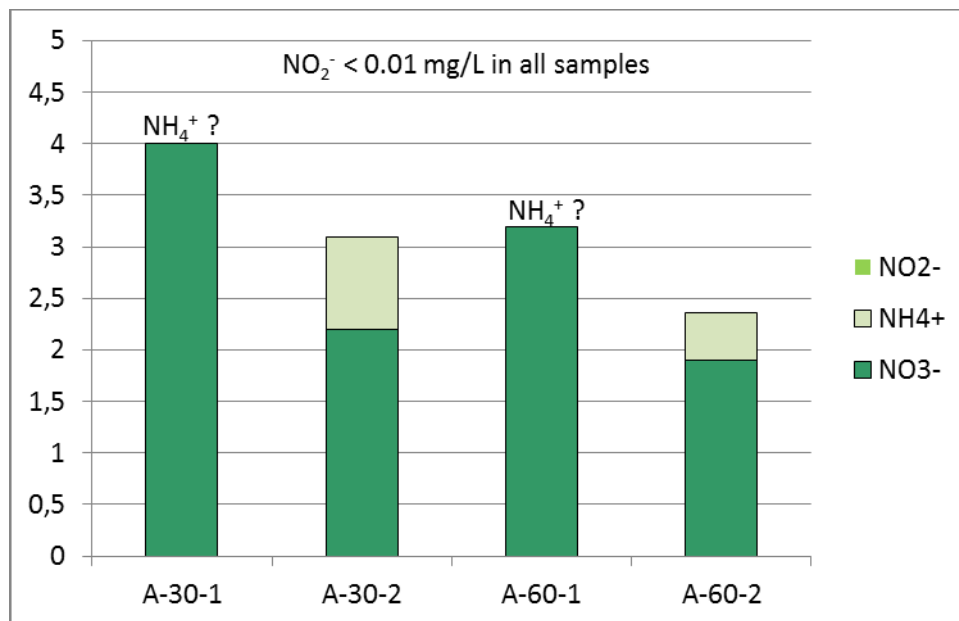
Figure 15 – Nitrogen concentrations in the vadose zone capsules (30 cm and 60 cm) from Section A

The concentration in hydrocarbons (HC) along the experiment shows values higher than the average tracer concentration, possibly due to the difficulty of making a good mixture of HC in the injected water. So, possibly the portion of the tracer injected in Section A had higher values than the mixture analysed. Nonetheless, the HC were retained in very small concentrations (10 mg/kg) in Melides soil (Table 8). A second peak can be seen.

In the last sample, taken 24 h after the tracer injection, the concentrations of all chemical parameters were similar to the initial values.

Table 8 – Results from the chemical analysis of soil samples collected after Experiment 1 finished

Designation	Soil (mg/kg DW)					
	NO_3^-	NO_2^-	NH_4^+	PO_4^{3+}	SO_4^{2-}	HC
A_30_Soil	<20	0.080	<0.5	<0.05	<0.1	10
A_60_ Soil	<20	0.090	<0.5	<0.05	<0.1	<10
B_30_ Soil	<20	0.135	<0.5	<0.05	<0.1	<10
B_60_ Soil	<20	0.134	<0.5	<0.05	<0.1	36
C_30_ Soil	<20	0.132	<0.5	<0.05	<0.1	70
C_60_ Soil	<20	0.077	<0.5	<0.05	<0.1	<10

Figure 16 presents the breakthrough curves obtained in the saturated water from the piezometer installed in <u>Section B</u>, in 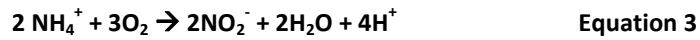which the first 60 cm of soil is a mixture of Melides soil (60%) and vegetal compost (40% with 65% organic matter), followed by Melides soil in the remaining depth.
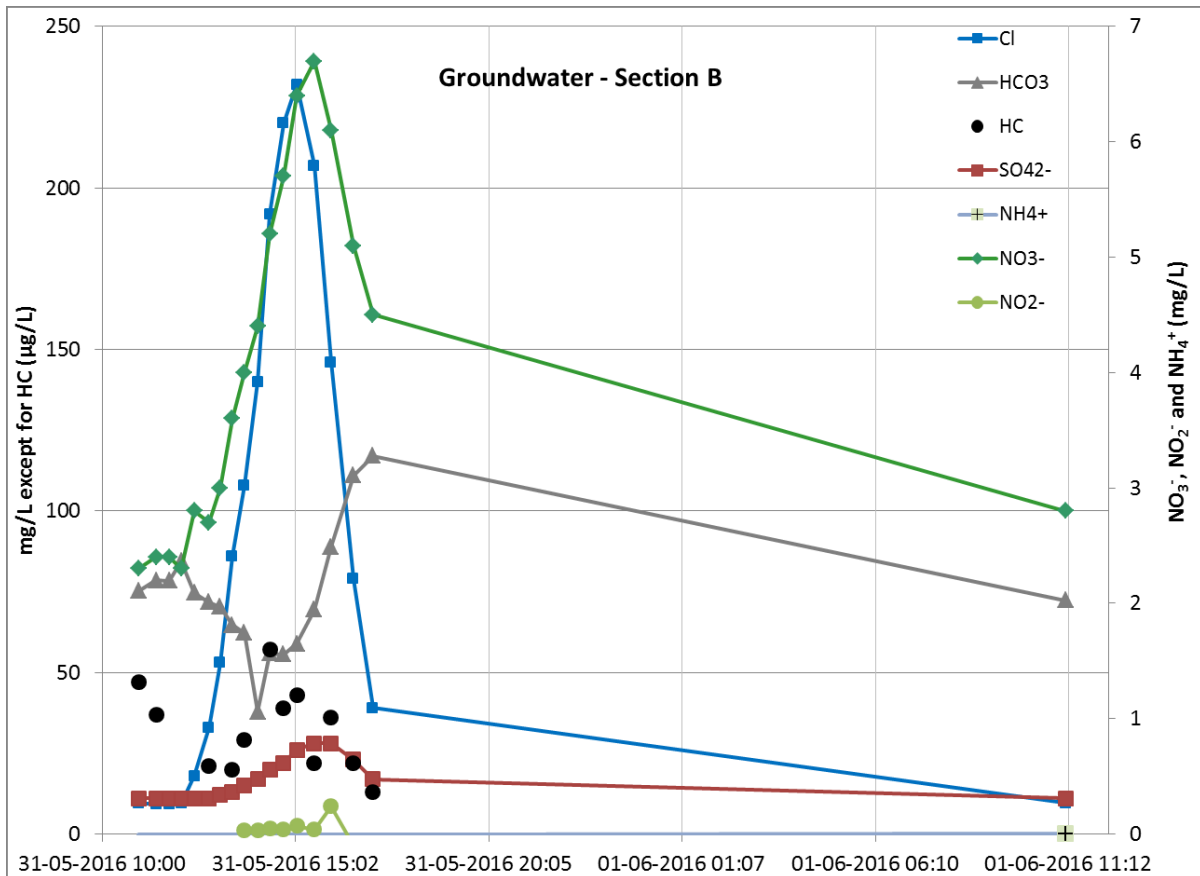
Figure 16 – Breakthrough curves obtained for the water samples from the Section B piezometer

The breakthrough curve for nitrates shows a higher dispersion when compared to Cl and to the results from Section A. Besides, the peak of nitrate arrival is 30 minutes slower (at 15:32) and has increased when compared to the initial tracer. The formation of nitrite (NO_2^-) (see also Figure 17), confirms the transformation of NH_4^+ into nitrite and nitrate through a nitrification process (see Equation 3 and 4 and Table 8). Besides, it is possible that some of the nitrate was subject to

denitrification in the presence of organic matter (CH_2O), producing bicarbonate (HCO_3^-) in the process:

$$5\ CH_2O + 4\ NO_3^- \rightarrow 2N_2\ (g) + 4\ HCO_3^- + CO_2 + 3H_2O \qquad\qquad \textbf{Equation 5}$$

The existence of a decrease in HCO_3^- concentrations, followed by a peak that is delayed compared to nitrate or NaCl, is a common phenomena in all three experiments. The peak should probably be a result of Equation 5, and the decrease might be due to some sorption phenomena.

Concerning the HC, the soil from Section B shows a better ability to retain these contaminants than Melides soil alone. The HC were retained close to 60 cm, but not in the first 30 cm (Table 8).

In the last sample, taken 24 h after the tracer injection, the concentrations of all chemical parameters were similar to the initial values.

Figure 17 – Nitrogen concentrations in the vadose zone capsules (30 cm and 60 cm) from Section B

Figure 18 presents the breakthrough curves obtained in the saturated water from the piezometer installed in <u>Section C</u>, with two vegetal compost layers of about 3 cm separated by 17 cm of Melides soil, followed by Melides soil in the remaining depth.

The breakthrough curve for nitrates shows lower maximum values when compared to Section B but also the formation of nitrite (NO_2^-) (see also Figure 19) through a nitrification process (see Equation 1 and 2). Denitrification is possible but the scape of N_2 to the atmosphere should be minor due to the lower permeability of the more organic layer. The retention of HC shows the best results when comparing the three sections. The concentration retained in the first soil layers is higher (Table 8) and therefore the concentration on the water is the lowest (Figure 18).

In the last sample, taken 24 h after the tracer injection, the concentrations of all chemical parameters were similar to the initial values.
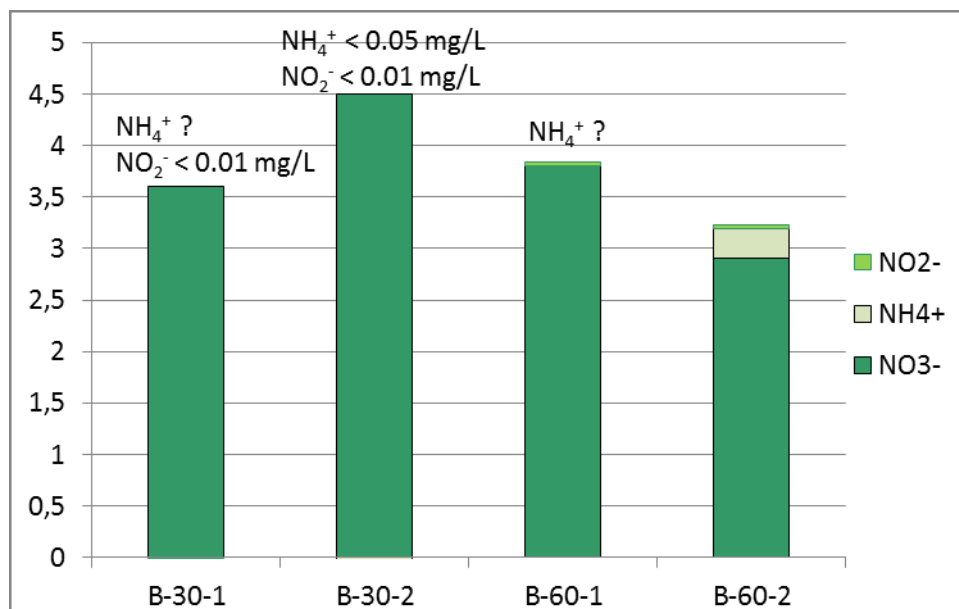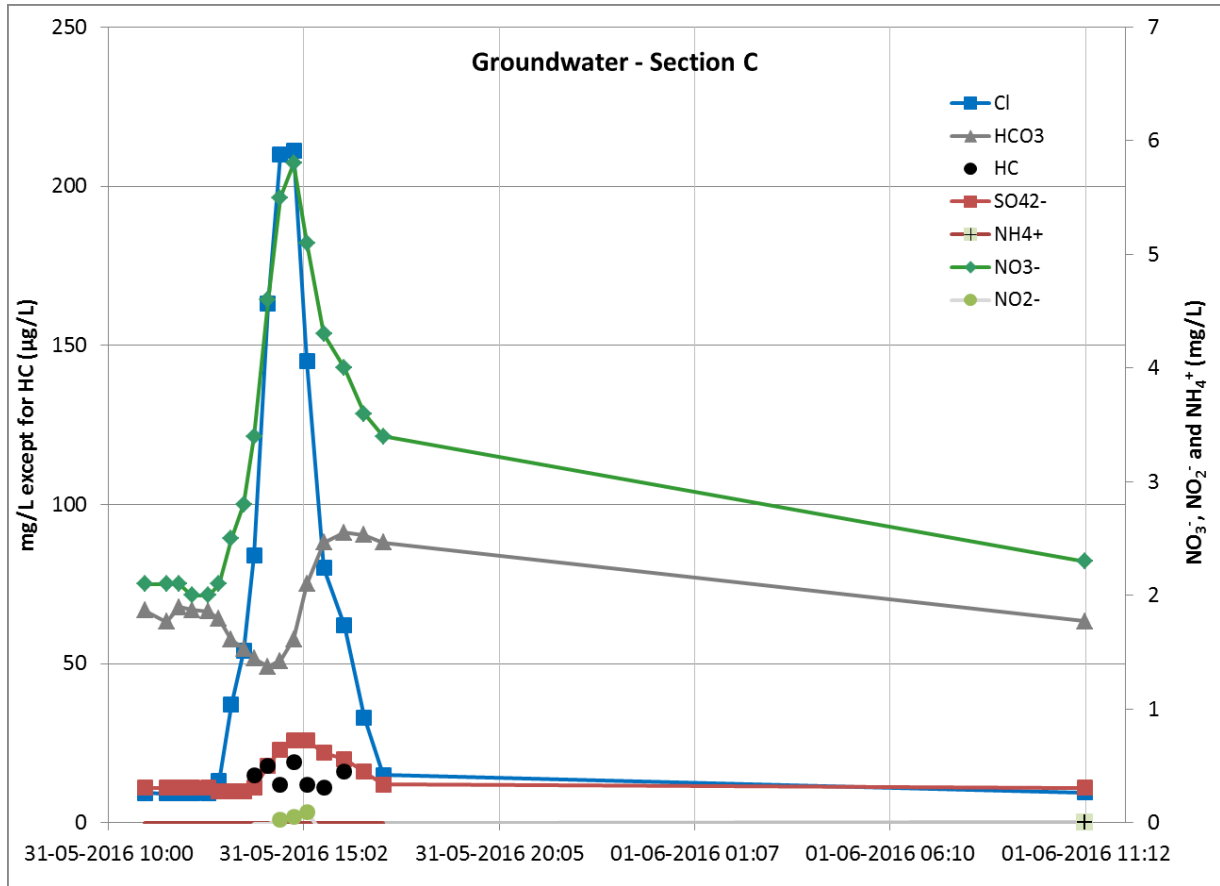
Figure 18 – Breakthrough curves obtained for the water samples from the Section C piezometer
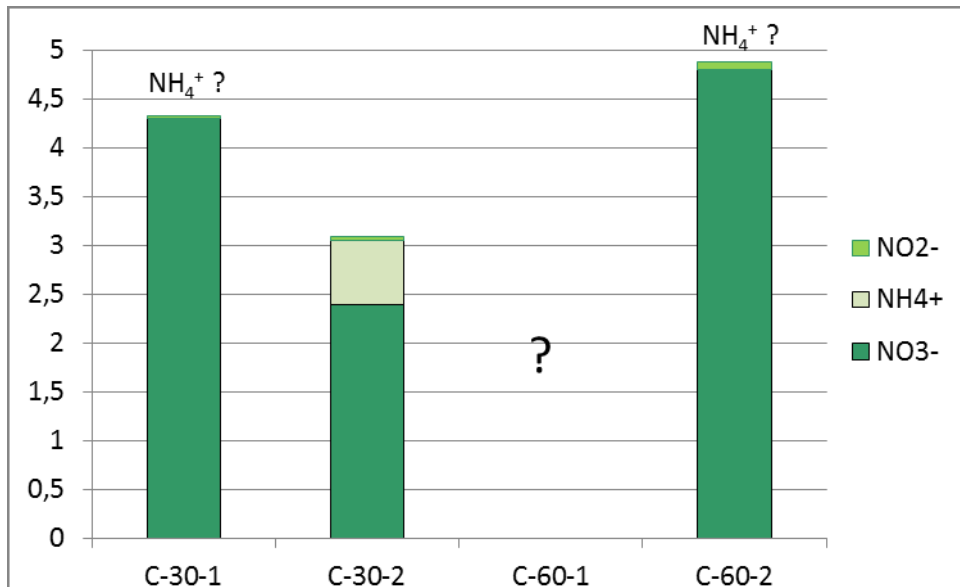
Figure 19 – Nitrogen concentrations in the vadose zone capsules (30 cm and 60 cm) from Section C

5.2 EXPERIMENT 2

Aiming to analyse the behaviour of same three soil mixtures (in Section A, B and C) in the case where the contaminants are slowly released, an Experiment 2 was carried out during 48 hours, between 12 AM of June 1st to 12 AM June 3rd. In this experiment the same tracer (fertilizer and NaCl) and concentrations were used, but no hydrocarbons (HC). Anyway the HC were analysed in the water sampled to see if any content still existed from the previous experiment. The tracer was placed on the soil surface in small grains (Figure 20) and it was slowly washed down by the irrigation process. It is expected that some soil contaminants from the previous experiment could still be attached to the soil.

Figure 20 – Detail of the soil surface with the tracer used for Experiment 2

Table 9 presents the main characteristics of Experiment 2 concerning the inflow and depth to the water table.

Table 9 – Main characteristics of Experiment 2

Date/time	Inflow (L/s)	Volume reading at counter (m^3)	Depth to the water table (m)	Notes
01-06-2016 11:55	0.079	-	1.22	Inflow restarted
01-06-2016 12:00	-	-	-	Experiment 2 starts / tracer released
01-06-2016 14:30	0.079	-	1.55	-
02-06-2016 08:00	0.09	-	1.57	-
02-06-2016 09:02	0.082	-	1.12	-
02-06-2016 11:52	0.082	-	0.78	-
02-06-2016 12:54	0.082	-	0.71	-
02-06-2016 14:30	0.083	-	0.81	-
02-06-2016 16:19	0.083	-	0.85	-
03-06-2016 12:00	-	-	-	Experiment 2 finishes
03-06-2016 14:45	0.069	10110.1	1.3	-
03-06-2016 16:46	0.075	10110.6	0.86	-
03-06-2016 17:05	0	-	0.77	Injection stopped / Divers removed

Figure 21 presents the results obtained from the CTD diver, for the depth to the water table and the electrical conductivity (EC). Although the inflow was kept approximately constant throughout the experiment (Table 9), the outflow was frequently changed while trying to adjust the depth to the water table to circa 0.8 m, the same value used for Experiment 1. This explains the water table changes observed in Figure 21. Concerning the EC registered in the piezometers, a much higher dispersion and a tail are observed in all sections, when compared to the corresponding section in Experiment 1. The disturbance caused by the soil sampling should be responsible for the disruption of Section C soil layers and a preferential flowpath should have been formed leading to a faster EC peak concentration and arrival in the Section C piezometer.

Comparing Experiment 1 and 2 tracer arrival, one can see that the liquid pulse tracer injection (Experiment 1) leads to a faster leaching, with an arrival to the piezometers approximately 4 hours after the experiment begins (Figure 13); and when the tracer is placed on the soil surface in small grains, the leaching is slower and the peak concentration starts to arrive 5 hours after the experiment and remains for much longer (Figure 21).
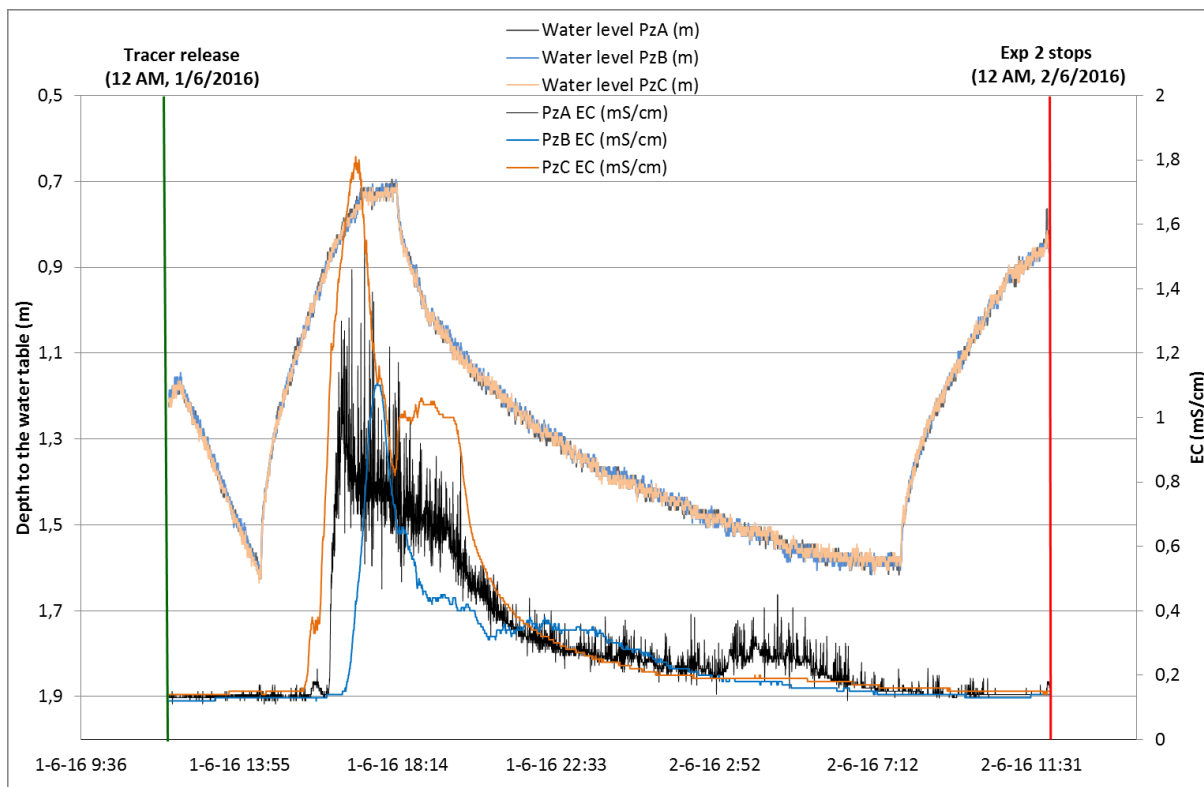
Figure 21 – Piezometric water level and electrical conductivity values in the three piezometers, Experiment 2

In addition to the continuous measurement of the EC, discrete samples were retrieved from the six vadose zone cups and the three piezometers, similarly to what was performed for Experiment 1. However, the samples were collected only at the end of each day and not hourly. Table 10 presents the water quality concentrations. The same designation procedure was used.

Table 10 – Results from the chemical analysis of water samples collected during Experiment 2

Designation	Day Hour	NO_3^-	NO_2^-	NH_4^+	Ca^{2+}	Mg^{2+}	Na^+	K^+	SO_4^{2-}	Cl^-	HCO_3^-	HC
Units						mg/L						µg/L
Vadose cups												
A-30-3	02-06	5.6	<0.01	2.1	-	-	-	-	21	251	45.5	-
A-60-3	02-06	1.8	<0.01	<0.05	-	-	-	-	11	18	51.4	-
A-30-4	03-06	1.9	0.01	0.9	-	-	-	-	11	10	46.2	-
A-60-4	03-06	1.7	<0.01	<0.05	-	-	-	-	11	10	54.5	-
Piezometers												
A-GW-19	02-06	1.9	<0.1	1.3	34	20	28	16	11	12	46.4	<10
A-GW-20	03-06	1.8	<0.1	0.51	21	6.6	11	4.9	11	9.9	48.3	<10
Vadose cups												
B-30-3	02-06	10	0.03	1	-	-	-	-	25	78	106	-
B-60-3	02-06	2.3	0.01	<0.05	-	-	-	-	11	187	76.1	-
B-30-4	03-06	3.6	0.02	0.2	-	-	-	-	11	10	-	-
B-60-4	03-06	1.9	<0.01	<0.05	-	-	-	-	11	11	67.1	-
Piezometers												
B-GW-19	02-06	3.6	<0.1	0.32	20	3.9	23	6	12	13	83.6	<10
B-GW-20	03-06	2.9	<0.01	0.25	24	3.6	11	4.2	11	9.6	76.3	<10
Vadose cups												
C-30-3	02-06	6.1	0.03	1.5	-	-	-	-	19	421	60.2	-
C-60-3	02-06	2.6	0.02	-	-	-	-	-	11	11	-	-
C-30-4	03-06	2.3	<0.01	0.18	-	-	-	-	11	14	55.5	-
C-60-4	03-06	2	0.01	-	-	-	-	-	11	10	-	-
Piezometers												
C-GW-19	02-06	2.6	<0.1	0.52	16	2.6	15	5	11	9.2	60.1	<10
C-GW-20	03-06	2.2	<0.01	0.27	21	2.8	9.3	2.5	11	11	63.8	<10

Figure 22 presents the results obtained for the nitrogen (N) cycle, namely nitrates (NO_3^-), nitrites (NO_2^-) and ammonia (NH_4^+). In all Sections A, B and C the highest concentrations of NO_3^- and NH_4^+ were observed in the first day (02-06-2016) and at the first vadose zone cup, 30 cm depth. In the cases where NH_4^+ analysis was possible, the concentration in the Cup at 60 cm was below the detection limit, although it is present in the piezometers water. Values for NO_2^- were very low, close to the detection limit.
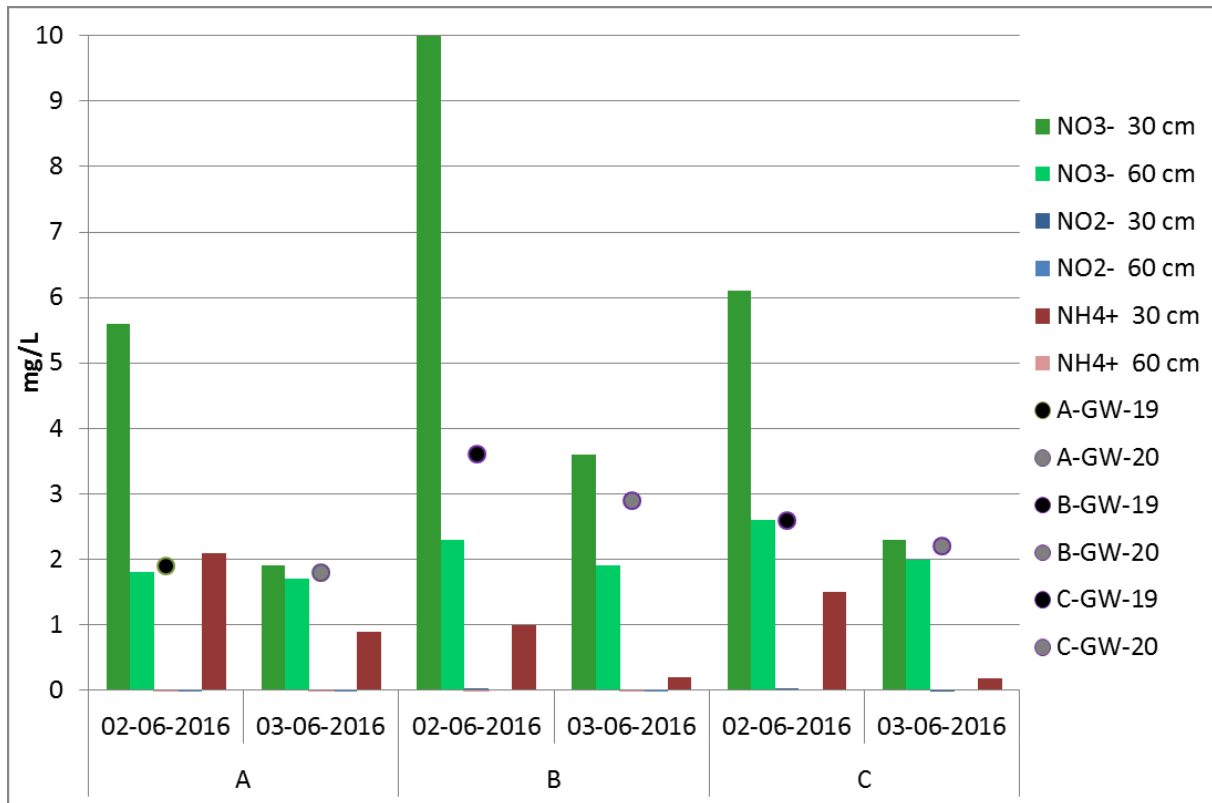
Figure 22 – Concentrations of N cycle in the water from the vadose (30 and 60 cm) and saturated (GW) zones

As could be seen in Experiment 1, also in Experiment 2 nitrification (Equations 1 and 2) occurs in the upper part of the soil (first 30 cm), with the presence of O_2. This process seems to be stronger in Section B, where the values for NH_4^+ are lower and for NO_3^- are higher. Besides, some denitrification should also occur in Section B forming HCO_3^- (Equation 3) (see Table 10).

No hydrocarbons were detected in the water sampled from the piezometers.

5.3 CONCLUSIONS

Comparing Experiment 1 and 2 results, it can be concluded that although there is a clear difference in the contaminants concentration throughout the experiment, after 48 hours the values are similar to the initial concentrations and equilibrium has been attained.

Nitrification (from ammonia to nitrate) and denitrification (from nitrate to gaseous N) seem to be the most common phenomena. Both are more likely to occur in the first soil layers due to the presence of oxygen and the possibility of N_2 gas to escape to the atmosphere. The presence of a more organic layer (Section B and C) favours denitrification and seems to be more effective in Section C (although this is not so clear in Experiment 2 due to the previous soil disturbance due to sampling).

The removal of hydrocarbons is clearly more effective for Section C.

6. NUMERICAL MODELLING

6.1 INTRODUCTION

FEFLOW finite element numerical model was used as a complementary method for understanding the behaviour of the tracers used. Each Section A, B and C was modelled using as input the data collected before and during the conducted experiments and, as a first approach, nitrogen cycle elements (nitrates, nitrites and ammonia) were used for flow and transport analysis.

Transient flow and mass transport simulations were run in vertical cross-sections considering a variably saturated media (Richard's equation). Only Experiment 1 was numerically modelled taking into account that the tracer was injected in a pulse solution and a considerable number of samples were collected with small time spacing between sampling. In Experiment 2, the small number of collected samples did not allow a comparison and analysis of tracer behaviour throughout the experiment.

Section 6.2 explains in detail input data while Sections 6.3 and 6.4 present and discuss the results obtained for each section.

6.2 INPUT DATA

All input data considered in the modelling process is summarized in Table 11, referring to the set of soil physical and hydraulic properties presented in the previous sections.

Table 11 – Input data for artificial aquifer FEFLOW models

Parameter			Section A	Section B	Section C	Ref.
Top section area (m^2)			1.0925	1.0925	0.96425	-
Height of section profile (m)			2.055	2.04	2.03	-
Total simulation time (d)				3		-
Soil parameters	K (m/d)	Natural soil		3.46		-
		Soil mixture	-	3.27	-	-
		OM layer	-	-	1.7	-
	n	Natural soil		0.38		-
		Soil mixture	-	0.38	-	-
		OM layer	-	-	0.4	-
Boundary conditions	Upper			Well BC		-
	Input BC volume (m^3/d)		2.877		2.538	-
	Lower			Fluid-flux BC		-
	Output BC permeability(m/d)		2.613		2.305	-
Solute parameters	Diffus. Coef. In Water (m^2/s)	NO_3^-		1.7		bionumbers.hms.harvard.edu
		NO_2^-		1.7e-9		
		NH_4^+		1.86		
	Long. Dispersivity			2		Šimůnek et al. (2013)
	Dispersivity Anis. Factor			0.1		-
Solute transport boundary condition	Upper			Concentration flux BC		-
	Concentration (mg/L)	NO_3^-		5.9		-
		NO_2^-		0.001		-
		NH_4^+		3.7		-

For each vertical cross-section a 500 element grid was generated (Figure 23), taking into account the dimensions as well as the distribution of the soil mixture and vegetal compost layers presented in Figure 8 and described in Section 4.3.
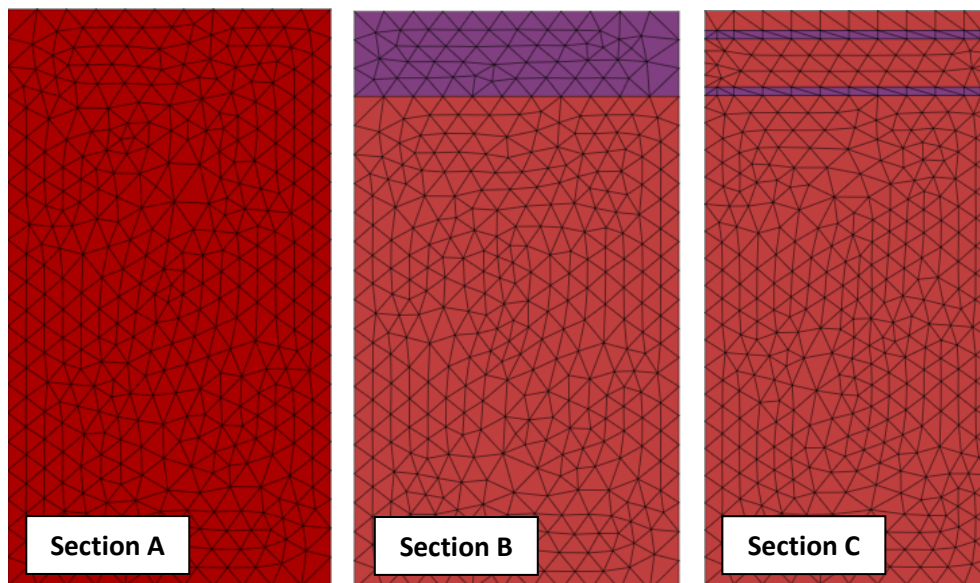
Figure 23 – Finite element grid for each modelled vertical section. Red cells represent natural soil while purple cells show the position of the soil mixture in Section B and vegetal compost layers in Section C

Concerning soil permeability, a set of considerations was taken into account:

- For the natural soil, in all sections, the average value of permeability used refers to that obtained for first day of the soil-column experiments previously conducted and briefly described in Section 3.4.

- Soil mixture permeability refers to the value obtained for a similar mixture artificially created and also tested in soil-column experiments.

- Vegetal compost layer permeability value is half of the K used for the natural soil. These layers weren't previously tested in soil-column experiments due to the large organic content (mainly decomposed roots, tree barks and leaves).

Porosity is considered the same for the natural soil (and was also determined from soil-column experiments) and for the soil mixture, and is slightly higher for the vegetal compost layers. This last assumption results from the composition of these vegetal compost layers with large organic decomposing plant parts.

A set of boundary conditions (BC) were established aiming to achieve the main water flow observed in the artificial aquifer cross-sections. At the top, a specific volume is injected through a Well BC. Input volume results from the proportional distribution of the injected volume to the different sections, taking into account that Section C top area is slightly smaller in comparison to Section A and B (Figure 8), therefore a smaller inflow volume is considered.

At the bottom, and considering the characteristics of the artificial aquifer outflow (Figure 8), a Fluid-flux BC was considered with drainage values equivalent to the injected values by the top area of each

section. This way the flux is continuous and it is possible to consider an equilibrium state between inflow and outflow.

Solute parameters were defined using data from previously conducted simulations (dispersivity anisotropy factor), bibliographic references (longitudinal dispersivity) and open databases (diffusion coefficient in water).

Finally, it is considered for the solute BC that a known concentration is injected at the top of each section. In this case, a Concentration flux BC was used giving the concentrations values at inflow determined by analysing the tracer solution used in Experiment 1 (for the exception of nitrites where a very low value was used).

The models ran, as it was referred previously, in transient state for 3 days (d), where t0 is the time where the sprinklers at the top of the artificial aquifer were opened. Tracer injection started at t = 0.96875 d and stopped at t = 0.99 d.

To understand the tracer concentration variations throughout the experiment, and along the vertical cross-sections, a set of observation points (OPs) were equally positioned on the grids (Figure 24) – OP1 as the first and uppermost point and OP6 as the lowest one.
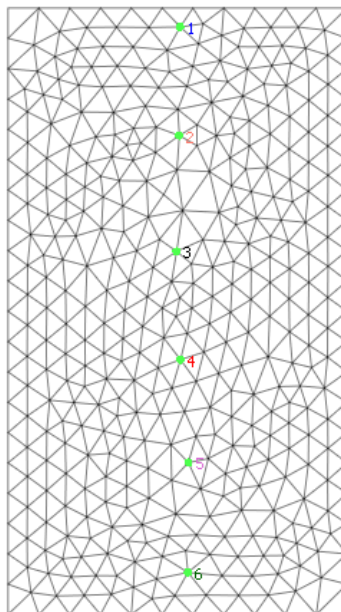
Figure 24 – Position of the observation points along each vertical section

6.3 RESULTS

Output results are represented in Concentration [mg/L] *vs* Time [d] for each tracer simulated by observation point. Each concentration curve has the colour or the specific observation point showed in Figure 24. It is important to keep in mind that the results presented at this point come from non-calibrated input data. Disclosing this information is important for the sake of result interpretation.

6.3.1   Section A

The results for the concentration variation through time for nitrates, nitrites and ammonia are represented in Figure 25, Figure 26 and Figure 27, respectively.

For nitrites and ammonia it is possible to observe the increase of concentration immediately after the tracer injection on the upmost observation point. This peak is followed by a fast decrease in concentration after the tracer injection stopped, assuming approximately at t = 1 d a concentration very close to 0 mg/L. Nitrates show, as expected from the inflow tracer solution concentration, higher concentration at the peak, compared to ammonia.

For these tracers, increase of concentration is also perceived in all other observation points, but only on OP 2 the concentration starts to decrease after t = 1 d.
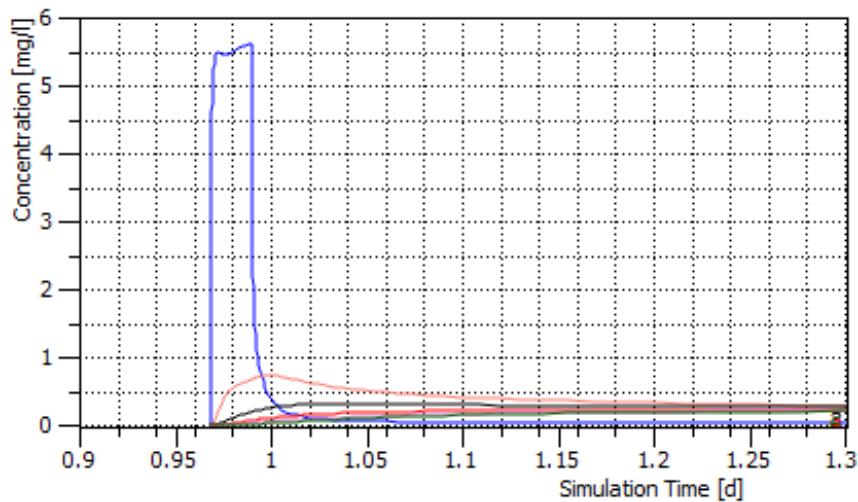

Figure 25 – Nitrates distribution throughout the experiment per observation point in Section A

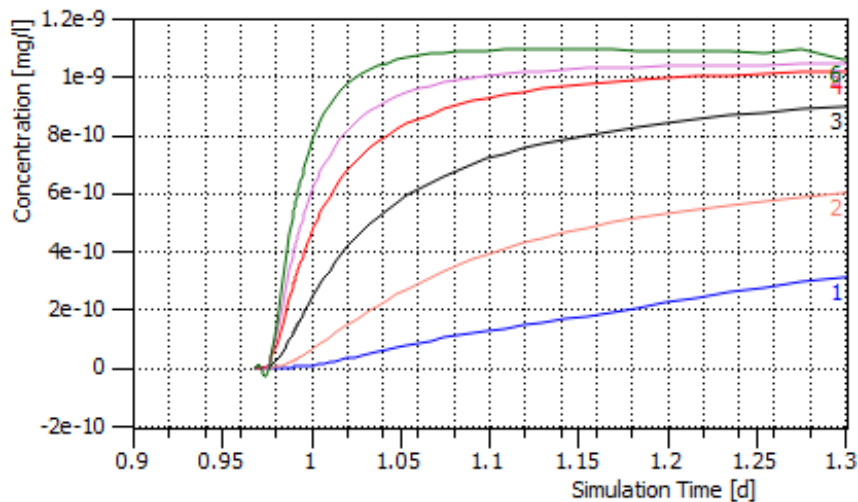Nitrites show very low concentration in all observation points.

Figure 26 – Nitrites distribution throughout the experiment per observation point in Section A

Figure 27 - Ammonia distribution throughout the experiment per observation point in Section A

6.3.2   Section B

The results for the concentration variation throughout time for nitrates, nitrites and ammonia are represented in Figure 28, Figure 29 and Figure 30, respectively.

In Section B, both nitrate and ammonia show a very similar behaviour to Section A, with a significantly immediate increase in concentration and the abrupt decrease after tracer injection stopped. Although the maximum value observed for both traces in OP1 is equal to that observed in Section A, it takes slightly more time to achieve it, possibly due to the difference in permeability between the soil mixture and the natural soil. This was also evidenced when comparing Figure 14 with Figure 16, although it refers to the values at the piezometers. However the increase of nitrate observed in Section B was not observed in the modelling.

For all the other observation points, a similar pattern to Section A is registered, and nitrites also show very small concentrations.

Figure 28 – Nitrates distribution throughout the experiment per observation point in Section B

Figure 29 – Nitrites distribution throughout the experiment per observation point in Section B
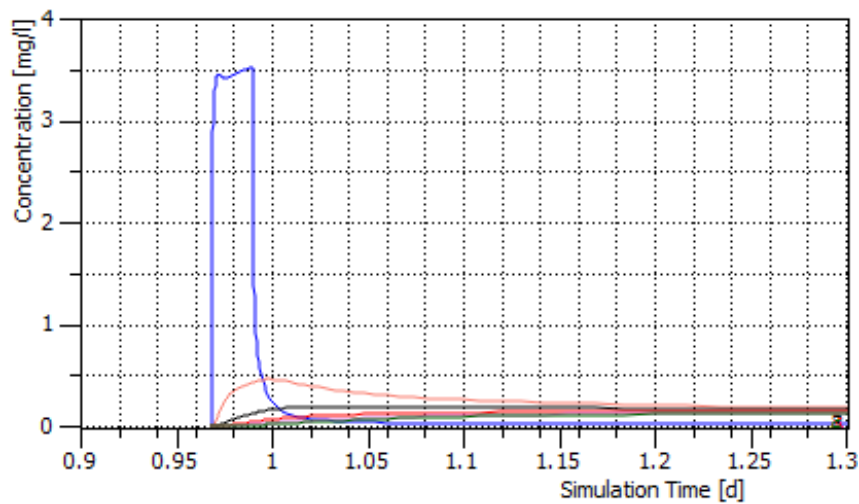

Figure 30 – Ammonia distribution throughout the experiment per observation point in Section B

6.3.3   Section C

The results for the concentration variation throughout time for nitrates, nitrites and ammonia in Section C are represented in Figure 31, Figure 32 and Figure 33, respectively.

Once again a fast increase in concentration in OP1 is observed for both nitrates and ammonia, although the curve is different from the other sections. The first vegetal compost layer (which has lower permeability) results in a very brief decrease in tracer concentration only to be followed by a second rapid increase. After the second vegetal compost layer the concentration of both tracers decrease again to low values (mainly in observation point 2, bellow de 2nd OM layer). Nitrites show once more very small concentrations as expected.
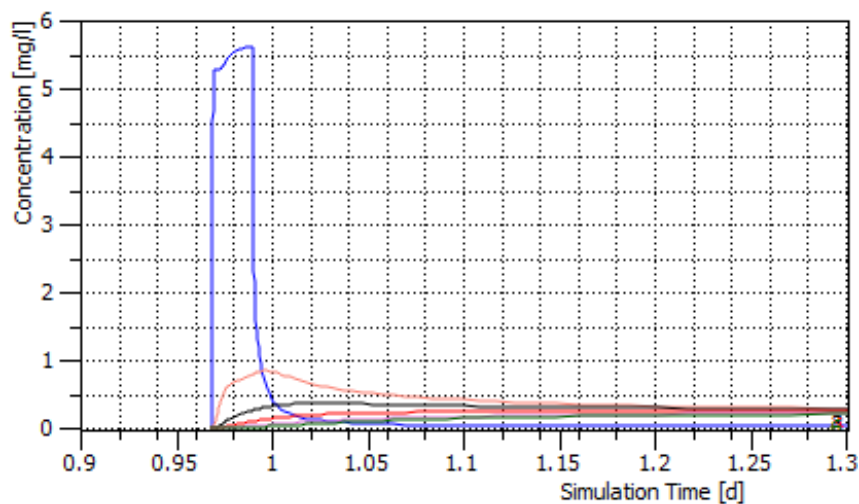
Figure 31 – Nitrates distribution throughout the experiment per observation point in section C
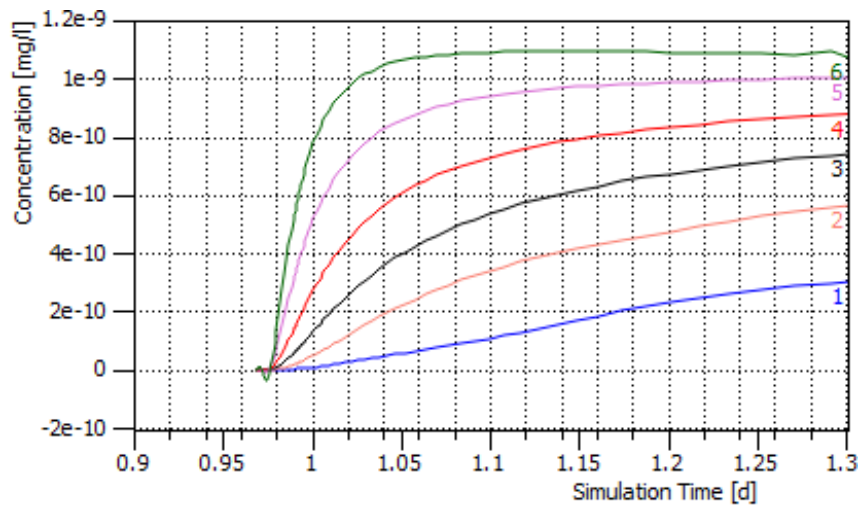

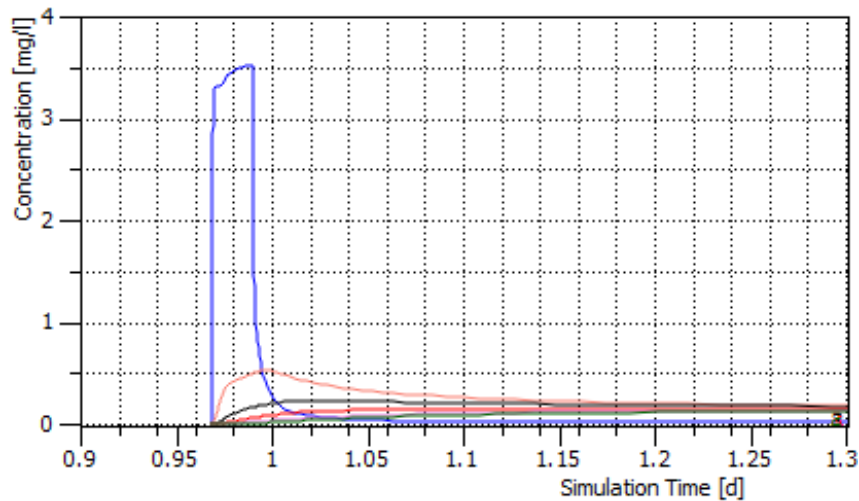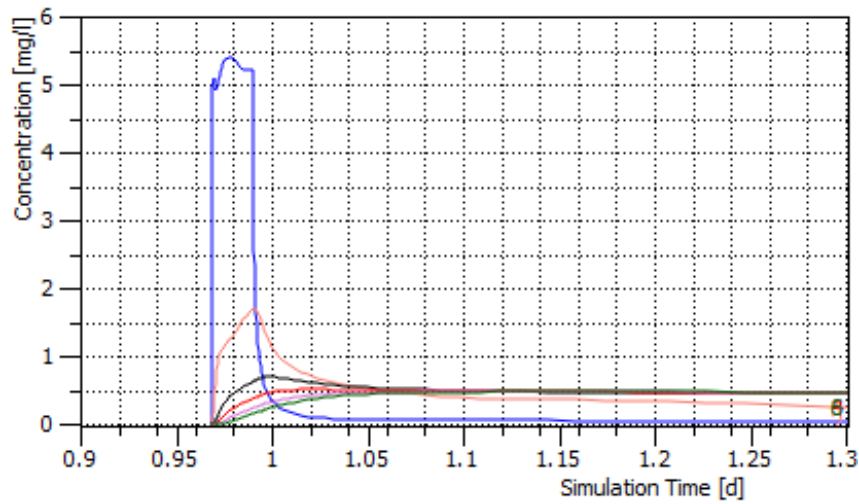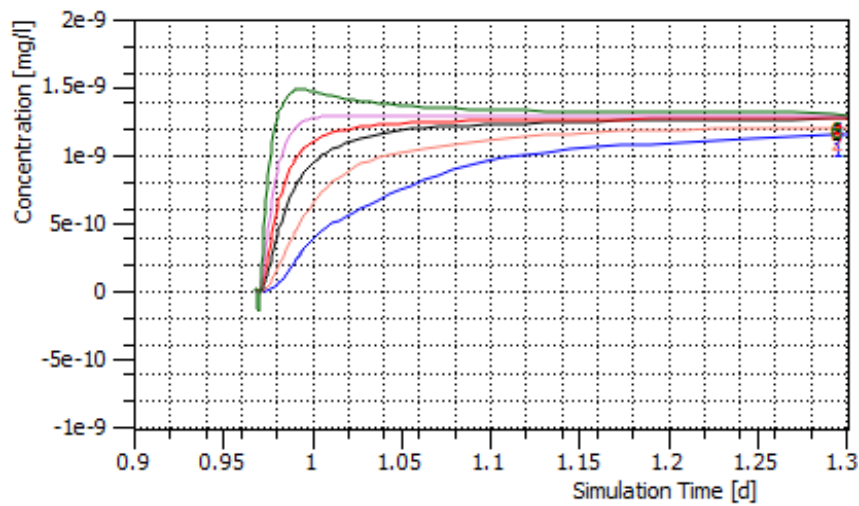**Figure 32 – Nitrites distribution throughout the experiment per observation point in section C**
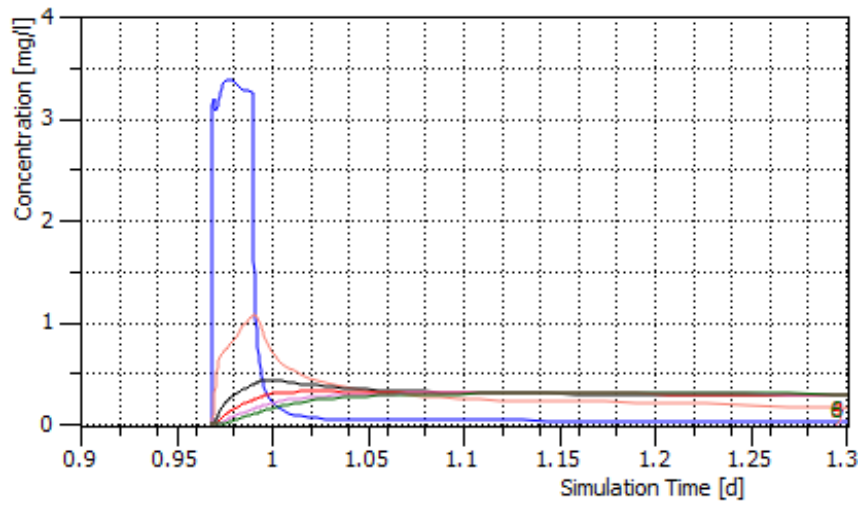

Figure 33 – Ammonia distribution throughout the experiment per observation point in section C

6.4 GENERAL RESULTS DISCUSSION

In general, the tracers considered are immediately dispersed at the uppermost part of all the vertical sections. Although smaller changes in tracer behaviour are observed due to the different hydraulic parameters of soil mixture and vegetal compost layers, the final outcome is similar in all sections.

While there are significant differences in the concentration behaviour in the uppermost part of all section, mainly for nitrates, is similar between what was observed during Experiment 1 and what was obtained by the numerical models. Significant differences were observed between model and reality in the lower part of all the vertical cross-sections where the concentrations of nitrates are several orders of magnitude higher than those calculated.

Nitrification process was not simulated, with degradation of nitrates to ammonia. If this was the case, a different behaviour should have been observed in the concentration *vs* time graphics, where nitrates peak is observed in the uppermost OPs, a second peak in the OPs situated in the middle of the vertical section OPs related to nitrites, and a final concentration peak in the lower OPs associated to ammonia.

A final note concerning the numerical modelling process: it's important to keep in mind that these results are preliminary, intended to understand the general behaviour of tracers in the physical sandbox model, as this case-study main focus was to gather experience on the physical modelling process and on their results. Later, if SAT-MAR is to be implemented in the reality of Melides DEMO site, there is plenty of room to further improve FEFLOW finite-element models.

7. FURTHER DEVELOPMENTS

7.1 SAT-MAR AREA NEEDED FOR TREATMENT

The main purpose of the physical sandbox experiments was to assess the ability of a SAT-MAR scheme to retain the contaminants (N and hydrocarbons) existing in the water from the rice paddy fields. Although the ability to denitrify (nitrate to N_2) is modest and more effective only in the first soil layer, the removal of total hydrocarbons seems effective.

In this section, a brief analysis of the potential implementation of a SAT-MAR scheme is done for Melides area. The aerial photography analysis allowed determining a total area of the rice paddy fields of about 1.6 km^2 (exactly 1.601084 km^2).

Figure 34 – Melides lagoon rice paddy fields area

According to Pereira (1989) (Http://www.oagricultor.com/bal_hid_arroz.htm) the water height within the paddy fields may vary between 5 cm, at the initial phase (seed), and 10 cm on the final development. Thus, the total volume retained in Melides lagoon beds can be determined accordingly to Table 12.

Table 12 – Total water volume in Melides paddy fields

	Water height (m)	Water volume (m^3)	hm^3
Initial phase (seed)	0.05	80054.2	0.080
Maximum development	0.1	160108.4	0.160
Average	0.075	120081.3	0.120

In order to identify the area needed for the SAT-MAR basins, a square basin prototype was envisaged with 1, 1.5 and 2 m depth (Table 13).

Table 13 – Basin area needed for SAT-MAR in Melides paddy fields

Basin depth (m)		1	1.5	2
	Basin area (m^2)			
Water volume (m^3)	80054.2	80054.2	53369.5	40027.10
	160108.4	160108.4	106738.9	80054.20
	120081.3	120081.3	80054.2	60040.65
	Side wall size (m)			
Water volume (m^3)	80054.2	282.9385	231.0183	200.0677
	160108.4	400.1355	326.7092	282.9385
	120081.3	346.5275	282.9385	245.0319

Considering the possibility of building the basins taking into account the values proposed in the above tables and a volume corresponding to the minimum height of water (5 cm), i.e. 80054 m^3, the following assumptions can be considered:

- Each basin with 100 m side wall size and 2 m high holds 20000 m^3 of water. So, to hold the minimum volume of 80054 m^3 four basins are required.

- Each basin with 150 m side wall size and 2 m high holds 45000 m^3 of water. So, to hold the minimum volume of 80054 m^3 two basins are required.

After visiting Melides lagoon (03/04/2013) and also using aerial photography, two distinct areas were selected as possible areas to place the SAT-MAR basins. They are relatively flat and situated between the paddy fields planting area and the lagoon, reducing the need for other hydraulic structures associated with water transfer for the infiltration basins. The total area of zone A is 44894 m^2 and area B is 59524 m^2.

Figure 35 – Areas available for the SAT-MAR basins at Melides

Figure 36 illustrates the possible arrangement of the square basins with different side wall sizes within the available areas.

Figure 36 – Possible location for the SAT-MAR basins at Melides (blue square is 100 m side and red square is 150 m side)

However, these basins would only have the ability to receive about 1/3 of the total volume of the rice paddy fields for a water blade height of 7.5 cm (about 120000 m^3) in the case of 100 m, and 3/4 of the total volume for the basins with 150 m side.

Another feature to consider is the water transfer needs from the ponds to the basins. For that, a Digital Terrain Model (DTM) was used and the paddy fields were divided in three subareas, according to the criteria established by Oliveira *et al*. (2012). Table 14 and Figure 37 present the subareas considered and their dimensions.

Figure 37 – Melides lagoon rice paddy fields subareas

Table 14 – Subareas dimensions at Melides lagoon rice paddies field

Subarea designation	Area (m^2)
Subarea A	649915.7285
Subarea B	885026.0677
Subarea C	66142.6949

If we take as an example the mean level of the paddy fields subarea A and the average level of the two available Areas A and B, it becomes clear that the water transfer to the basin cannot be made by gravity (Table 15), making a pumping mechanisms necessary. However this conclusion is strongly dependent on the accuracy of the DTM, so a topographic study is necessary in order to obtain accurate dimensions of the entire area.

Table 15 – Elevation needed for the water transfer from the paddy fields to the SAT-MAR basins

	Elevation (m)		
	Average	**Minimum**	**Maximum**
Area available A	13.57	9.52	20.67
Area available B	10.09	7.79	15.98
Subarea A (paddy fields)	5.58	1.35	15.45
Subarea B (paddy fields)	9.88	3.00	20.61
Subarea C (paddy fields)	19.42	17.52	21.15

Using the same methodology as for the total area of the paddy fields, the volume of water retained in the beds for different stages of growth is presented hereinafter.

Subarea A

Table 16 presents the water volume existing in subarea A.

Table 16 – Melides paddy fields Subbasin A water volume

	Water height (m)	Water volume (m^3)	hm^3
Initial phase (seed)	0.05	32495.786	0.0325
Maximum development	0.1	64991.573	0.0650
Average	0.075	48743.680	0.0487

The basin area and the side wall size area presented in Table 17.

Table 17 – Melides paddy fields Subbasin A area needed for SAT-MAR

Basin depth (m)		1	1.5	2
		Basin area (m^2)		
Water volume (m^3)	32495.786	32495.79	21663.86	16247.89
	64991.573	64991.57	43327.72	32495.79
	48743.680	48743.68	32495.79	24371.84
		Side wall size (m)		
Water volume (m^3)	32495.786	180.266	147.187	127.467
	64991.573	254.934	208.153	180.266
	48743.680	220.780	180.266	156.115

Subarea B

Table 16 presents the water volume existing in subarea B. The basin area and the side wall size area presented in Table 17.

Table 18 – Melides paddy fields Subbasin B water volume

	Water height (m)	Water volume (m^3)	hm^3
Initial phase (seed)	0.05	44251.303	0.0443
Maximum development	0.1	88502.607	0.0885
Average	0.075	66376.955	0.0664

Table 19 – Melides paddy fields Subbasin B area needed for SAT-MAR

Basin depth (m)		1	1.5	2
		Basin area (m^2)		
Water volume (m^3)	44251.303	44251.30	29500.87	22125.65
	88502.607	88502.61	59001.74	44251.30
	66376.955	66376.96	44251.30	33188.48
		Side wall size (m)		
Water volume (m^3)	44251.303	210.360	171.758	148.747
	88502.607	297.494	242.903	210.360
	66376.955	257.637	210.360	182.177

Subarea C

Table 16 presents the water volume existing in subarea C.

Table 20 – Melides paddy fields Subbasin C water volume

	Water height (m)	Water volume (m^3)	hm^3
Initial phase (seed)	0.05	3307.135	0.0033
Maximum development	0.1	6614.269	0.0066
Average	0.075	4960.702	0.0050

The basin area and the side wall size area presented in Table 17.

Table 21 – Melides paddy fields Subbasin C area needed for SAT-MAR

Basin depth (m)		1	1.5	2
		Basin area (m^2)		
Water volume (m^3)	3307.135	3307.135	2204.756	1653.567
	6614.269	6614.269	4409.513	3307.135
	4960.702	4960.702	3307.135	2480.351
		Side wall size (m)		
Water volume (m^3)	3307.135	57.508	46.955	40.664
	6614.269	81.328	66.404	57.508
	4960.702	70.432	57.508	49.803

7.2 WATER BALANCE

7.2.1 Precipitation and evapotranspiration

The average month precipitation values (Oliveira *et al.*, 2011) were used for running BALSEQ_MOD, from a series of 30 years (Table 22). The average rainfall during the crop season was calculated from this set of precipitation values (Table 22).

Table 22 – Average monthly precipitation values in Melides

Month	Precipitation (mm)
October	85.22
November	95.02
December	94.75
January	78.58
February	60.63
March	45.69
April	57.08
May	40.93
June	10.09
July	2.43
August	3.8
September	30.84
Annual	605.05
Crop season	114.33

Considering that the production of rice extends from April to August, the respective cumulative rainfall and the volumes that occur in the total area of paddy field were estimated in the respective subareas and basins proposed (Table 23).

Table 23 – Cumulative rainfall and volumes values for Melides paddy fields area

Designation		Area	Volume (area* precipitation 0.11433 m) accumulated for the rice cycle (April - August)	
		m^2	hm^3	m^3
Total area		1601084	0.183	183051.934
Subarea A		649915.7285	0.074	74304.865
Subarea B		885026.0677	0.101	101185.030
Subarea C		66142.6949	0.008	7562.094
Basin (2m height)	100 m	10000	0.001	1143.300
	150 m	22500	0.003	2572.425

The precipitation values represent an important component of the water balance in terms of area of paddy fields being essential to quantify the amount of water that is retained and the amount that infiltrates.

Another important element is the evapotranspiration. From the reference evapotranspiration data used by Oliveira *et al*. (2011) the average monthly accumulated a series of 30 years (1966-1996) was determined. If it is considered that the actual evapotranspiration is equal to the crop coefficient for that culture times, than the reference evapotranspiration value for this parameter has a value of 337.9 mm for the summer months (Table 24).

So it turns out that in the rice paddy fields areas, and in this specific case, the evapotranspiration values during the summer season are much higher than the rainfall, and so the evapotranspiration volume necessary for the proper growth of the crop must come from abundant irrigation. For the dimensioning of the basin one should consider only the volume needed to fill the beds, in which for the case of subarea A is 48743.67 m^3. Water infiltration from the paddy field was not considered in these calculations.

Table 24 – Cumulative average month evapotranspiration values for Melides paddy fields area

Month	Month average	Kc*	ETR (mm)
January	18.35	0.65	11.93
February	25.77	0.65	16.75
March	48.82	0.65	31.74
April	73.82	0.65	47.98
May	108.99	0.65	70.84
June	125.64	0.65	81.67
July	71.64	0.65	46.57
August	139.75	0.65	90.84
September	100.14	0.65	65.09
October	68.49	0.65	44.52
November	37.03	0.65	24.07
December	22.76	0.65	14.79
Crop season	519.84	ETo (Summer)	337.9

*(according to Allen *et al.*, 1998 the average Kc in water without turbidity and in a mild climate is 0.65)

7.2.2   Basin infiltration capacity

Dividing the total volume required to fill Subarea A up to the average height of 7.5 cm (48743.67 m^3) using two infiltration basins with 150 m side (area of 22500 m^2), a first water level of 1.8 m per basin is needed. If the previously calculated value of 114.46 mm / summer precipitation value is considered, for the same area with 2572 m^3 / basin a water depth of 0.114 m is calculated. The total water height by basin is 1.194 m.

To determine the daily volume that passes through the bottom section of the infiltration basin (150 x 150) one needs to consider the permeability of the soil media where infiltration is made. Section 3.4 presents the results obtained in the lab for these Plio-Pleistocene sands. The average Darcy permeability ranged from 0.9 to 4.8 m/d.

Considering an effective porosity of 38% (see Section 3.3), applying the Darcy formula and considering that the hydraulic gradient is equal to 1 (dx = dh = 1.194 m), the infiltration capacity of the basin was determined.

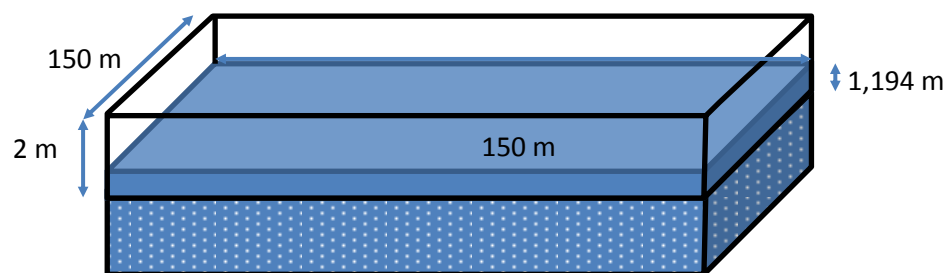$$Q = V (K. i) a . n \qquad\qquad \textbf{Equation 6}$$

Where:

Q – Flowrate
V – velocity
K – permeability
 I – hydraulic gradient
a – cross-section area
n – porosity

Thus, under ideal conditions (ignoring the phenomenon of clogging the pores), a basin with side wall dimension of 150 m has the ability to daily infiltrate from 7695 m^3 to 41040 m^3, which represents about 16% to 84% of the volume total water needed for paddy field Subarea A (Table 16).

BIBLIOGRAPHY

Leitão, T.E.; Oliveira, L.S.; Lobo Ferreira, J.P.; Vilhena, J.; Almeida, A.; Tomé, M.; Pires, A.M. (2012) - Análise Integrada da Qualidade da Água e dos Ecossistemas na Bacia Hidrográfica da Ribeira de Melides. 11.º Congresso da Água – Valorizar a água num contexto de incerteza, organizado pela APRH, Porto, 6-8 de Fevereiro de 2012, 15 pp.

Lobo Ferreira, J.P., Novo, M.E., Oliveira, L. (2013) - Análise da Contribuição das Fontes Poluentes para a Carga Total de Nitratos e Fosfatos que Afluem à Lagoa de Melides por Transporte Subterrâneo. 11º SILUSBA "A Cooperação para a Água", Maputo, Moçambique.

Monteiro, J. P.; Chambel, A.; Martins, J. (2008) - Conceptual and Numerical Flow Model of the Sines Aquifer System (Alentejo, South Portugal). International Groundwater Symposium. International Association of Hydraulic Engineering and Research (IAHR). Istanbul-Turkey. p.38 (abstract) and doc. elect. CD-Rom 9 pp.

Novo, M.E.; Oliveira, L.G.S. (2014) - Uso de cenários de alterações climáticas para previsão do estado de aquíferos e EDAS. Caso de Estudo: Melides. Revista Recursos Hídricos. Associação Portuguesa dos Recursos Hídricos. Volume 35, Nº 2, novembro 2014.

Oliveira, L., Martins, T., Lobo Ferreira, J.P., Oliveira, M.M., Novo, M.E., Leitão, T.E. (2012) - Água, Ecossistemas Aquáticos e Atividade Humana – Projeto PROWATERMAN. Contributos para o Desenvolvimento de Medidas para uma Gestão Sustentável dos Recursos Hídricos no Sul de Portugal. Relatório 153/2012-NAS, 44 pp.

Oliveira M.M.; Oliveira L.S. (2012) - Water, aquatic ecosystems and human activity project PROWATERMAN. 5th Thematic Report. Recharge and direct runoff assessment of Querença-Silves aquifer system catchment area. Report 180/2012-NAS. LNEC, pp. 108. In Portuguese: Água, Ecossistemas Aquáticos e Atividade Humana. Projeto PROWATERMAN. Quinto Relatório Temático - Estimativa da recarga e do escoamento direto na área de drenagem do sistema aquífero Querença-Silves.

PEREIRA, L. A. (1989) - Gestão da Rega do Arroz. Instituto Superior de Agronomia. Tese de doutoramento, Lisboa.

Šimůnek, J., Šejna, M., Saito, H., Sakai, M., van Genuchten, M. (2013) The HYDRUS 1.D Software Package for Simulating the One-Dimentional Movement of Water, Heat, and Multiple Solutes in Variably-Saturated Media – Version 4.17. Department of Environmental Sciences, University of California, 308 pp.